

THE UNIVERSITY OF MANITOBA

THE COMPLIANCE OF CONTRACTING SKELETAL MUSCLE

by

BERNARD HARVEY BRESSLER

A THESIS

SUBMITTED TO THE FACULTY OF GRADUATE STUDIES

IN PARTIAL FULFILMENT OF THE REQUIREMENTS FOR THE DEGREE

DOCTOR OF PHILOSOPHY

DEPARTMENT OF PHYSIOLOGY

WINNIPEG, MANITOBA

October 1972



To my wife, Sandra.

## ACKNOWLEDGEMENTS

I am greatly indebted to my supervisor, Dr. Norman F. Clinch, who has been a constant source of guidance and encouragement throughout the study and the preparation of this manuscript.

I wish to thank Dr. Arnold Naimark, former Head of the Department of Physiology, for giving me the opportunity to study in his department. Special thanks are also due to Dr. Ken Hughes, Acting Head of the Department, for his active interest in my education.

My appreciation is also extended to Vic Tennant for many worthwhile discussions and for his help with the derivation of the equation used for correcting the sarcomere widths. Expert secretarial help of my wife Sandra and Mrs. Kathy MacDonald is gratefully acknowledged.

This work was completed while the author was in receipt of a University of Manitoba Fellowship and subsequently, a Pre-Doctoral Fellowship from the Muscular Dystrophy Association of Canada. The cost of this research was defrayed from funds provided by the Medical Research Council of Canada to Dr. Norman Clinch.

## ABSTRACT

Skeletal muscle contraction is described most frequently by the two-component model which puts an inert, non-linear elastic element in series with a shortening generator, the contractile component. The characteristics of the contractile element are described by its ability to shorten and develop force at different speeds depending on the load. The series elastic component is characterized by tension-extension curves which provide a measure of the instantaneous stiffness of an active muscle. Recent evidence has cast doubt on the series elastic component as being an inert, constant element during contraction. We obtained tension-extension curves for toad (Bufo bufo) sartorii at various times during initial force development and from maximum tetanic tension at different muscle lengths ( $l_0 < l < l_0$ ), by giving a single controlled release ( $> V_{max}$ ) to zero tension. The stiffness of the active muscle was found to be a function of the muscle length, decreasing in the same way as the isometric force decreases, as the muscle is stretched above body length. At lengths below  $l_0$ , there was a similar decrease in instantaneous stiffness with a fall in isometric tetanic tension, though the stiffness was always somewhat higher than the force. Furthermore, the tension-extension curves were found not to be invariant in time during the initial development of tension, but rather, were related to the developed force. If we assume that the force a muscle produces depends on the maximum number of parallel cross-links formed on activation, then our results are consistent with the idea that a large part of the series compliance resides in the sarcomeres,

most likely in the cross-bridges themselves. Moreover, the fall in stiffness at short lengths rules out the possibility that the major source of an active muscle's compliance is in the unbonded I-filament.

The force-velocity curve for the toad sartorius was measured either by allowing the muscle to shorten against different loads or by giving a controlled velocity release to an isometrically contracting muscle at preset times during a contraction. Both methods gave similar results.

Finally a light diffraction technique was used to determine the sarcomere width of the toad sartorius at various muscle lengths.

## TABLE OF CONTENTS

	Page
LIST OF FIGURES	
LIST OF TABLES	
I. INTRODUCTION	1
II. REVIEW OF LITERATURE	
1. The Visco-Elastic Theory	3
2. Emergence of a New Interpretation of Skeletal Muscle Contraction	6
3. The Two-Component Model	10
a) The Force-Velocity Component	10
b) The Series Elastic Component	12
i) Historical Background	12
ii) Series Elasticity in the Sarcomeres	16
III. METHODS	
1. Elasticity Experiments	22
a.) Materials	22
b.) Experimental Procedure	27
c.) Analysis of Data	28
d.) Active State and Instantaneous Elasticity	29
2. Force-Velocity Experiments	29
3. Diffraction Patterns of Toad Sartorii	31

	Page
IV. RESULTS	
1. Force-Velocity Experiments	37
2. Elasticity Experiments	37
a.) Active State and Instantaneous Elasticity	40
b.) Velocity of Release	44
c.) Tension-Extension Curves at Long Lengths	47
d.) Tension-Extension Curves at Short Lengths	54
e.) Initial Development of Force	59
3. Laser Experiments	69
V. DISCUSSION AND SUMMARY	
Discussion	74
Summary	83
VI. BIBLIOGRAPHY	85
VII. APPENDIX	94

## LIST OF FIGURES

Figure		Page
1	A visco-elastic model	5
2	Isometric myograms: Jewell and Wilkie (1958)	15
3	Block diagram of apparatus	25
4	Response of loudspeaker system	26
5	Experimental set up for force velocity experiments	30
6	Record of a controlled release experiment	32
7	Diffraction pattern of toad sartorius	33
8	Force velocity data	39
9	Tension-extension curve from $P_0$ in a contracting muscle	41
10	Active state experiment	43
11	Tension-extension curves at different release velocities	45
12	Tension-extension curves at long lengths	48
13	Means and standard deviations of stiffness and tension at long lengths	53
14	Relation between maximum stiffness and tetanic force at long lengths	55
15	Tension-extension curves at short lengths	58
16	Relation of stiffness to length below $l_0$	60
17	Comparison of maximum stiffness and peak tetanic tension to length below $l_0$	61



Figure		Page
18	Relation between maximum stiffness and tetanic force at short lengths	62
19	Relation between stiffness and initial development of force	67
20	Effective tension-extension curve versus eleven others	68
21	Distribution of sarcomere widths	70
22	A comparison of tension-length curves	71
23	Experimental and predicted relation between stiffness and force at long lengths	77
24	Isometric myograms: calculated and observed	81

## LIST OF TABLES

Table		Page
I	Definitions of frequently used terms	23
II	Values of the force velocity constants for the toad sartorius from isotonic and controlled velocity release experiments	38
III	Stiffness values for the toad sartorius at $l_{\max}$	42
IV	Stiffness and tension values for the toad sartorius at long lengths	50
V	Stiffness and tension values for the toad sartorius at short lengths	56
VI	Stiffness and tension values for the toad sartorius during the initial development of force	64
VII	Calculated stiffness at different sarcomere lengths if all the stiffness were in the I-band	95
VIII	Calculated stiffness at different sarcomere lengths if all the stiffness were in the cross-bridges	97

## I. INTRODUCTION

For many years skeletal muscle contraction has been thought of in terms of the two-component model introduced by A.V. Hill (1938). In an isometric contraction of a whole muscle (or a single muscle fiber) a contractile element in the muscle is thought of as actively shortening against, and extending an inert, non-linear, elastic body, the series elastic component. The rate of development of force in an isometric twitch or tetanus was thus determined only by the velocity of shortening of the contractile element and the stiffness of the SEC (Hill, 1938). Over the past fifteen years, however, it has become increasingly clear that the two-component model is an oversimplified view of how muscles work (Jewell and Wilkie, 1958; Ritchie and Wilkie, 1958; Civan and Podolsky, 1966; Armstrong, Julian, and Huxley, 1966; Hill, 1970; Schadler, Steiger, and Ruegg, 1971). Recent work by Huxley and Simmons (1970, 1971a, 1971b) has shown that sarcomeres have much more complicated mechanical properties which could be interpreted as showing that most of the series compliance lies in the cross-bridges.

The object of the present research was to examine more closely the compliance properties of contracting muscle. Our results show that the stiffness of an isometrically tetanised muscle is a function of muscle length, decreasing in the same way as the isometric force decreases, as the muscle is increasingly shortened or stretched from the optimum length. Furthermore, just as the tension-extension curve of an active muscle cannot be regarded as invariant with respect to length, neither is it invariant in time during the initial

development of isometric force. These results are also compatible with the idea that a substantial amount of the muscle's compliance resides in the sarcomeres, most likely in the cross-bridges themselves.

## II. REVIEW OF THE LITERATURE

## 1. The Visco-Elastic Theory

In 1922, A.V. Hill demonstrated in flexor muscles of the human arm that the work done in shortening a fixed distance during a maximal voluntary contraction decreased as the speed of the shortening increased. This fundamental response of skeletal muscle was interpreted in terms of the visco-elastic theory. In this model the active muscle was analogous to a stretched spring that was attempting to shorten. Furthermore, there was assumed to be a considerable increase in the internal viscosity of the active muscle so that any shortening was opposed by a frictional force proportional in magnitude to the velocity of shortening,  $v$ . Thus only when  $v = 0$  was the full force of the elastic network expressed externally. The isometric force was given the symbol  $P_0$ . For  $v > 0$  the developed force  $P$  was always less than  $P_0$  according to the relation

$$P = P_0 - kv$$

where  $v$  is taken as positive for decreasing length and vice versa (see also Lupton, 1923; Hill, Long and Lupton, 1924). In order to rule out the possibility that the relation of force to speed of shortening was dependent on some regulatory mechanism inherent in the nervous system, experiments were done on isolated frog muscles stimulated directly (Gasser and Hill, 1924). Releases and/or stretches at different speeds from the plateau of isometric tetani indicated that the active muscle was considerably less extensible than unstimulated (resting) muscle. Furthermore the observed behavior of a muscle due to an imposed length change was reproducible experimentally with a visco-elastic

model using a thin rubber pipe and a mixture of vaseline and oil, the viscosity of which could be changed by altering the temperature. With both the muscle and the rubber tube, an instantaneous release caused a drop in tension below the equilibrium state of the new length followed by a gradual rise to the new equilibrium level. Gasser and Hill also made direct determinations of changes in muscle viscosity by recording the damping effects of an active muscle on the oscillations of a flat steel spring. They concluded that, qualitatively at least, the results were consistent with the idea that an active muscle was analogous to a stretched spring in a viscous medium.

Although no evidence was available from biochemical studies to support or refute the visco-elastic theory, the total heat measured when the length of a muscle was altered passively was attributed in part to a degradation of the mechanical energy of the muscle due to internal frictional and viscous forces (Hill and Hartree, 1920).

Levin and Wyman (1927) using a much improved myograph were able to obtain very accurate tension-length curves from muscles released or stretched at different velocities. A significant finding was that the tension-length curves were not linear but exponential. During a constant velocity release there was a large initial drop in tension which then fell more gradually as the movement went on. Furthermore, the total work done by the muscle (the area under the tension-length curve) as a function of the speed of shortening was an S-shaped curve. Both these findings were not predicted by the Gasser and Hill model in



which there was a single damped spring surrounded by a viscous fluid (Fig. 1a).

If such a system was subjected to a quick release there would be an instantaneous fall to zero tension. Moreover there would be a linear relationship between the work done in shortening a given distance and the speed of shortening.

Therefore Levin and Wyman (1927) proposed a "two-part viscous-elastic system of which one elastic element is free and the other damped", to explain their results (Fig. 1b)

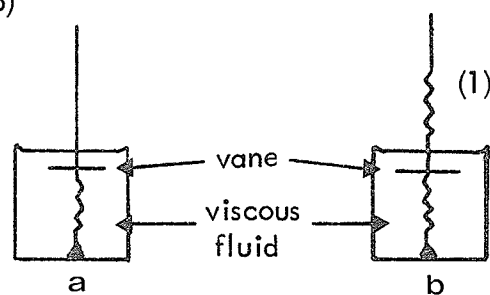


Fig. 1

With such an arrangement, a sudden length change to an isometrically contracting muscle was immediately taken up by the undamped element (1). This would destroy the equilibrium between the two springs. When the release stopped, the viscous-elastic element would continue to shorten, stretching the purely elastic element until the equilibrium tension was reached. It was interesting that the redevelopment of tension was seen to follow the same time course as the initial development of force (Gasser and Hill, 1924; Levin and Wyman, 1927). Finally, Gasser and Hill showed that both the initial development and redevelopment of tension exhibited the same changes with a change in temperature. This further supported the concept of an abrupt increase in viscosity of the stimulated muscle.

## 2. Emergence of a New Interpretation of Skeletal Muscle Contraction

The visco-elastic theory remained the most suitable model to describe skeletal muscle contraction (see for example Boukaert, Capellen and de Blende, 1930) until the work of Fenn and Marsh appeared in 1935. They used isotonic contractions to measure the speed of shortening of the damped elastic element against different loads. In an isotonic situation, i.e. at a constant load, the length of the undamped elastic element remained constant so that any observed shortening must be due to the damped element alone. They did not see a linear relationship between force and shortening velocity as would be expected from a simple visco-elastic system. The velocity of shortening was related exponentially to the force and could be expressed by the formula  $P = P_0 e^{-\phi v} - kv$  where  $\phi$  is the coefficient of tension loss,  $k$  is the coefficient of viscosity,  $P$  is the force,  $v$  is the velocity of shortening, and  $P_0$  is the maximum force developed in an isometric tetanus. Moreover, Fenn (1923, 1924) had pointed out ten years earlier that the heat production by the sartorius in an isotonic contraction usually exceeded the isometric heat, and always did so for loads greater than zero. The muscle was analogous to a chain and windlass in which "... every link of the chain which is wound up involves the expenditure of so much energy at the moment of winding". This was inconsistent with the view that the activated muscle initially contained a fixed amount of elastic potential energy which could be released during contraction. Fenn's results were largely ignored until Fenn and Marsh published the first real evidence of a force-velocity relation

which they felt could not be explained by a purely mechanical system. They proposed that muscle had some intrinsic chemical control system which regulated energy production and accounted for the regulated shortening of the contractile component.

These findings were subsequently confirmed by Hill (1938) studying the heat production of isolated frog muscle. In the isotonic situation where a muscle was allowed to shorten a fixed distance under different loads or different distances under the same load, the initial rise of heat increased in proportion to the distance shortened and was independent of the speed of shortening. This led to the concept of the 'shortening heat' given by  $ax$  where  $a$  is a constant and  $x$  is the distance shortened. Thus during the initial heat produced (up to the time of relaxation) the total energy liberated is,

$$E = A + ax + Px$$

where  $A$  is the activation heat (the initial heat, prior to the relaxation heat, seen in an isometric twitch),  $ax$  is the extra heat produced due to muscle shortening, and  $Px$  is the mechanical work done in lifting the load. In an isotonically contracting muscle the total extra energy liberated,  $E_x$  (in excess of the activation heat) can be expressed as,

$$\begin{aligned} E_x &= ax + Px \\ &= (P + a)x \end{aligned}$$

The rate of extra energy liberation is,

$$\frac{dE_x}{dt} = \frac{dax}{dt} + \frac{dPx}{dt}$$

a and P are not changing with time so now,

$$\frac{dE_x}{dt} = P \frac{dx}{dt} + a \frac{dx}{dt}$$

and,

$$\dot{E}_x = (P + a) v$$

Hill then showed that the rate of extra energy liberation varied linearly with the load (or,  $P_o - P$ ). That is,

$$(P + a)v = b(P_o - P)$$

where a and b are constants; b has units of velocity and a has the dimensions of force, and  $P_o$  is the maximum tetanic force at body length. If we add ab to both sides of the above equation and rearrange it so that the right hand side contains only constant terms we obtain Hill's characteristic equation,

$$(P + a)(v + b) = (P_o - a) b$$

This predicts that the force-velocity relation should be part of a rectangular hyperbola ( $x \cdot y = k$ ). This equation turned out to be in excellent agreement with the experimental force-velocity data of Fenn and Marsh and other workers, including Hill himself. Moreover the characteristic equation has been successful in fitting force-velocity data from an enormous variety of other muscles of all types and from many phyla of the animal kingdom. Finally the good agreement between the mechanical and thermal values of the constants a and b were taken

to confirm Hill's results.

Hill modified the two-part viscous-elastic model in which, now, the inert, undamped elastic element was placed in series with a shortening generator that was governed by intrinsic chemical events and whose properties could be described by the characteristic equation.

The elastic properties of unstimulated muscle are regarded as due to the connective tissue surrounding the muscle (epimysium) and around the muscle fibers (perimysium and endomysium) (Banus and Zetlin, 1938) and possibly the sarcolemma at sarcomere lengths beyond  $3.0\mu$  (Casella, 1950; Natori, 1954; Podolsky, 1964; Rapoport, 1972). Together these constitute a third component, the parallel elastic component. The PEC accounts for the appearance of resting tension seen when a sartorius muscle is stretched beyond the resting length (Hill, 1950a).

Katz (1939) tested the validity of the two-component model by attempting to predict the shape of the experimentally obtained isometric myogram from an experimentally derived P-V relation and predictions about the muscle's dynamic stiffness. The equation used by Katz was:

$$2.3 \times (1 + a/P_o) \times \log_{10} \frac{1}{1 - P/P_o} - P/P_o = t \times b/C$$

where  $t$  was the time interval from the start of tension rise,  $C$  was the total amount of elastic lengthening, and  $a/P_o$  and  $b$  were the constants from Hill's characteristic equation describing the force-velocity curve. The calculated

curves appeared to always rise faster than the experimental ones. The degree of success for an accurate prediction depended on the assumptions made about the dynamic stiffness of the series elastic element and the values of  $a$  and  $b$  from the characteristic equation. Katz suggested that the elastic tissue parts did not follow Hooke's law exactly, but more likely, their stiffness increased with increasing force.

The relationship between stiffness and force was determined experimentally by Buchthal, Kaiser and Knappeis (1944), and Buchthal and Kaiser (1944) using the technique of sinusoidal oscillations to an isometrically contracting muscle. These authors supported the idea of increasing stiffness with force showing, moreover, that this relation was linear. They showed that during contraction the muscle becomes more compliant with an increase in temperature. They interpreted their results as reflecting some property of molecular linkages within the muscle. Their findings can be extended to suggest a time and force dependent compliance within the sarcomeres. Unfortunately the orthodox view of an inert, series compliance caused this work to be overlooked for many years.

### 3. The Two-Component Model

#### a) The Force-Velocity Component

The most fundamental mechanical relationship of an active muscle is the decrease of shortening velocity with increasing load (see Hill, 1922; Levin and Wyman, 1927; Fenn and Marsh, 1935; Hill, 1938; Wilkie, 1950; Katz, 1939; Abbott and Wilkie, 1953; Abbott and Lowy, 1958; Sonnenblick, 1962;

Huxley, 1957; Julian, 1971). The energetics of the force-velocity relation were worked out by Hill (1938, 1949) (reviewed in section 2). His studies provided a characteristic equation that was remarkably consistent with results from mechanical experiments. Various other equations have been proposed for the force-velocity relation (see Hill, 1965, pg. 137) though Hill's remains the most widely used, perhaps because its derivation from energy flux data makes it seem less arbitrary than the others.

It is considered beyond the scope of this report to discuss the full implications of the P-V relationship (for a good review see Hill, 1965; Hill, 1970; Wilkie, 1950; and Caplan, 1966). However, I would like to mention some work that is relevant to the results presented in this thesis.

Abbott and Wilkie (1953) and Matsumoto (1967) have shown that Hill's force-velocity equation is valid for lengths other than  $l_0$  ( $l < l_0$ ). The constants  $a/P_0$  and  $b/l_0$  remain fixed providing the original equation is modified to take into account the change in  $P_0$  at different lengths. However, Gordon, Huxley, and Julian (1966b) have proposed that this relation does not really hold because in their experiments they consistently found that the velocity of shortening declined faster than the force at lengths below about  $1.9\mu$ . But above the plateau of the tension-length curve the velocity of shortening was nearly constant in spite of a decrease in maximum tension.

## b) The Series Elastic Component

### i) Historical Background

The concept of an undamped series elasticity in skeletal muscle was introduced by Levin and Wyman (1927) (see section 1). Evidence for the existence of an SEC was derived from mechanical experiments and it was assumed to be largely in the tendons (Hill, 1950b). The practical importance of the series elastic component is that it acts as a buffer. A muscle, on activation, would attempt to exert its full force against the inertia of the limb or an external mass and would probably tear. With the series compliance present, the full force of the muscle develops more slowly, allowing the mechanical energy in the SEC to be used in producing a final velocity greater than that at which the contractile component itself can shorten (Hill, 1939, 1950b).

Jewell and Wilkie (1958) provided convincing evidence for the presence of an undamped passive series elasticity while studying the shortening of a maximally tetanized muscle (at  $l_0$ ) when it was suddenly allowed to shorten under a constant load. The shortening record showed a very quick initial change in length followed by a steady shortening, the velocity of which, like the early length step, depended on the load. The rapid length change was considered to be entirely due to the release of the series elastic component (see also Sandow's review, 1961).

Hill (1950b) established the technique of giving a single controlled release ( $V > V_{\max}$ ) to zero force from the peak of an isometric tetanus to obtain



the tension-extension curve of the series elastic component in frog and toad *sartorii*. The change in force during the release plotted against the change in length provided a tension-extension curve from which the muscle's instantaneous compliance (mm/gwt) or its reciprocal, instantaneous stiffness (gwt/mm) could be measured. For convenience load and extension are used rather than stress (gwt/cm<sup>2</sup>) and strain (length change/length) to describe the stress-strain properties of contracting muscle. A suitable way of comparing the physical properties of the series elastic component in different muscles is to compare the magnitude of release, as a percent of  $l_0$ , needed to reduce the tension to zero from  $P_0$ . This is also a measure of the total amount of stretch produced in the SEC as the muscle develops maximum isometric tension. The total series compliance of Hill's frog muscles (*Rana temporaria*) was found to be about 4% of the body length. During the early days of quick releases (Gasser and Hill, 1924) a release of at least 10% was needed to reduce the tension to zero. In these experiments a large fraction of the series compliance was in the recording equipment, thread, etc. With account taken of the stray compliance, the actual series compliance in frog muscles was reported by Jewell and Wilkie (1958) to be rather small, about 2% of the body length. Recent work on toad (*Bufo bufo*) *sartorii* indicated that a release of 1% to 1.5% was required to reduce the tension to zero from the peak of an isometric tetanus (Clinch and Bressler, unpublished). In cat papillary muscle estimates of the series compliance range from 6% (Abbott and Mommaerts, 1959) to 10% (Sonnenblick, 1962, 1964).

Recently Parmley and Sonnenblick (1967) have shown cardiac muscle to be stiffer (4% to 5%) than previously reported. Stephens and Kromer (1971) have measured a series compliance of 7.6% for tracheal smooth muscle in the dog. The significance of these findings is seen when considering the energetics of a contracting muscle. If a muscle has a more compliant series elasticity, then the contractile element will have to do more work in stretching out the SEC than in a less compliant muscle.

Attempts by numerous investigators to predict the shape of the experimentally obtained isometric myogram from experimental force-velocity curves and tension-extension curves of the SEC has usually been less than satisfactory (Katz, 1939; Ritchie and Wilkie, 1958; Jewell and Wilkie, 1958). In the work of Jewell and Wilkie (1958) for example, great care was taken to measure the force-velocity curve and the tension-extension curve of the same muscle in order to calculate the shape of the isometric myogram from the following relations:

$$\frac{dP}{dt} = \frac{dx}{dt} \cdot \frac{dP}{dx} \quad (1)$$

$$t(P) = \int_0^P \frac{1}{\frac{dx}{dt} \cdot \frac{dP}{dx}} \quad (2)$$

As can be seen from their fig. 7 which has been reproduced here as Fig. 2, the calculated curve always rises more quickly than the experimental one. The source of the discrepancy may have been related to errors in the force-velocity curve, errors in the tension-extension curves or a fault in thinking

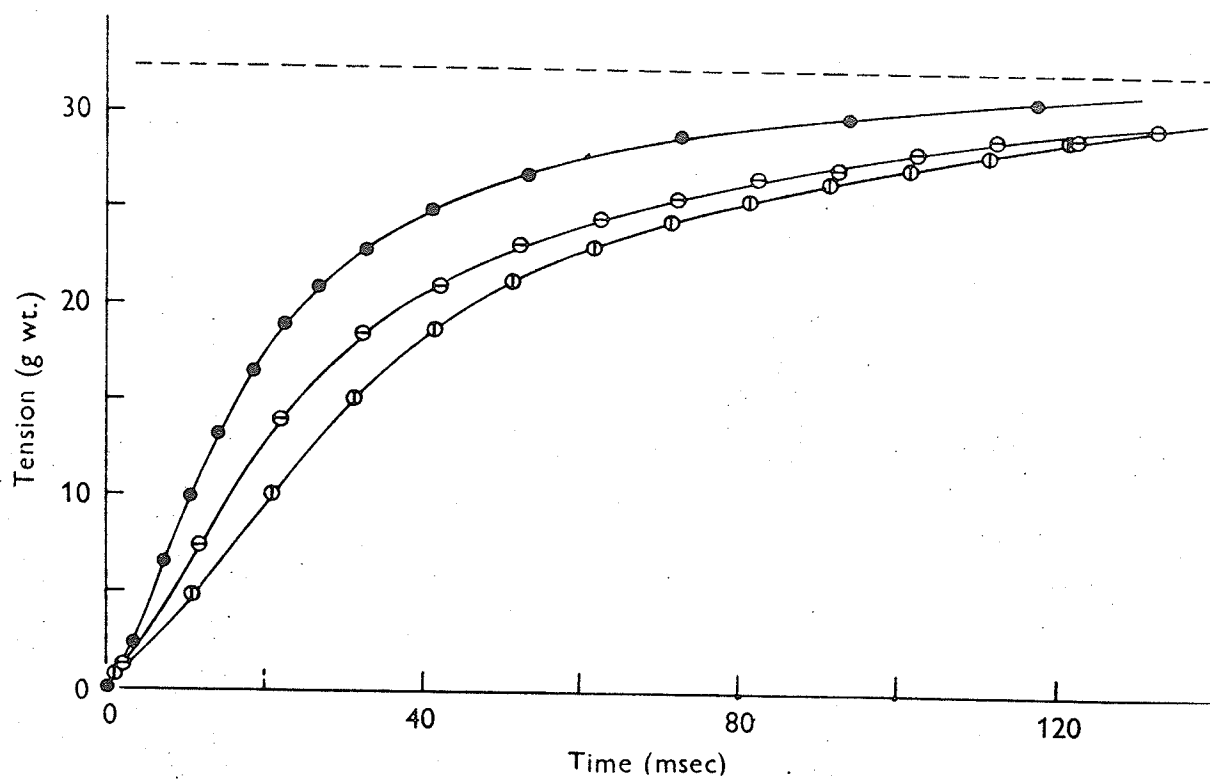


Figure 2: Isometric myograms reproduced from Jewell and Wilkie (1958). Open circles; the observed myograms:  $\odot$ , initial rise of tension;  $\ominus$ , redevelopment of tension after a quick release at 0.7 sec. Solid circles: curve of rise of tension calculated from the force-velocity and load-extension curves.

that a muscle at  $l_0$  can be strictly considered in terms of the two-component model. The question of whether the force-velocity data obtained from an isotonically contracting muscle can be considered to represent the contractile component under isometric conditions was answered by Jewell and Wilkie (1958) who concluded that the velocity of shortening was an instantaneous function of the load, within the limits of error in their experiments. Changes in velocity followed sudden changes in force with a delay of no more than 6 msec.

Wilkie (1956) measured the properties of the series elastic component at various times during a muscle twitch. His results indicated that the SEC exhibited roughly constant properties throughout a contraction; moreover, "... the site must be located in a region that was not subject to the profound change which occurs in the contractile proteins during activity". Parmley and Sonnenblick (1967) reported a similar finding of a constant series elasticity in cat papillary muscles.

## ii) Series Elasticity in the Sarcomeres

Hill (1951a) showed that placing an external compliance in series with a muscle produced a delay and a reduction in the maximum tension developed. The converse experiment of eliminating the external compliance has been done by Gordon, Huxley, and Julian (1966a) using their spot-follower device which constantly monitors the length of a middle segment of the muscle. In this instance it seems reasonable to suppose that a series elasticity may still be present in those areas of the myofilaments not actively engaged in tension

development. One theory of muscle contraction suggested that the muscle shortened and developed tension as a result of coiling of the thin filaments (Podolsky, 1959, 1961). However, A.F. Huxley and Niedergerke (1954) and H.E. Huxley and Hanson (1954) demonstrated that the length of the myofilaments remained constant during an isometric contraction. The change in length of the I-band during an isotonic contraction was due to sliding of the filaments relative to each other as tension was developed. Internal shortening was presumed to take place in an isometric contraction as well, as the contractile component stretched out the series elastic element. The constancy of the filament lengths has been confirmed by Page and H.E. Huxley (1963) in electron-micrographs of fully contracted muscle. In two independent studies Elliott, Lowy and Millman (1965) and H.E. Huxley, Brown and Holmes (1965) used low angle X-ray diffraction and showed no changes in the myosin and actin filament lengths in living toad and frog muscles during an isometric contraction. More recently Huxley and Brown (1967), again using a sensitive X-ray diffraction method, have shown only a 0.2% increase in the length of the thin filaments and a 1% increase in the periodicity of the A-filaments during an isometric contraction.

The cross-bridges, however, are not excluded as a possible source of compliance in the sarcomere. Civan and Podolsky (1966) studied the contractile properties of single fibers or small muscle bundles from frog and toad semitendinosus. If a single muscle fiber (or whole muscle) contracting isometrically

was suddenly released from  $P_0$  and allowed to shorten against a load  $P < P_0$ , there was a delay before the shortening velocity reached the level predicted by the P-V relation. This was in contradiction to the instantaneous change of velocity with load described by Jewell and Wilkie (1958) but supported A.F. Huxley's (1957) prediction of as much as a 28 msec. delay. This non-steady shortening was taken to represent the cyclic activity of the cross-bridges between the actin and myosin filaments. The time taken for the steady shortening to be reached had a large temperature coefficient suggesting a chemical rather than a physical process. Civan and Podolsky suggested a time-dependent compliance within the sarcomere, most likely to be found in the cross-links. This could be made consistent with A.F. Huxley's (1957) model by postulating additional properties for the elastic connection between the cross-link head and the myosin backbone. Furthermore, in Huxley's scheme the cross-links exerted force over distances as great as  $156A^\circ$  which makes an elastic connection probable.

D.K. Hill (1968) reported the presence of a short range elastic component in resting frog and toad sartorii. With stretches of up to 0.2%  $l_0$  at velocities of 10 - 100  $\mu$ /sec. there was a sharp, almost linear rise in the resting tension. The slope of this rise was taken to represent the elastic modulus of the short-range elastic component (SREC). When the stretch exceeded about 50  $\mu$  an "elastic limit" was reached, and then as further stretch occurred the tension was maintained as a constant "frictional resistance" which dropped to zero quite soon

after the stretch stopped. The elastic modulus of the SREC ( $7.4 \text{ kg/cm}^2$ ) was small in comparison to the elastic modulus of the filaments (estimated by D.K. Hill as  $> 50 \text{ kg/cm}^2$  at a developed tension of 2 gm). Thus the magnitude of the stretch was too small to produce any significant change in length of the filaments. This implied that the two sets of filaments might be sliding past each other and the resistance to stretch may be from the material between the filaments. Hill observed, further, that hypertonic solutions caused the resting tension to rise by about  $0.1 P_o$ . Although this was most likely a contracture, as suggested by Homsher and Briggs (1968), Hill interpreted this as representing the "filamentary resting tension". Moreover he proposed that even in the normal resting muscle some of the cross-links formed were producing the filamentary resting tension and were the ones responsible for the short range elastic component.

The work mentioned up to this point describes results which suggest that the two-component model is an oversimplified view of how muscles work. The remainder of this section deals with the experiments of A.F. Huxley and R.M. Simmons who have shown, recently, that sarcomeres have much more complicated mechanical properties which can be interpreted as showing that most of the series compliance lies in the cross-bridges. In the first series of experiments Huxley and Simmons (1970) showed that when an active muscle was suddenly released the tension dropped instantaneously and then recovered to an intermediate value in about 2 msec. followed by a more gradual redevelopment. This suggested an undamped elastic element in series with a damped one. Huxley

and Simmons (1971a) studied this quick phase of the series elastic component in single muscle fibers at different lengths beyond the rest length. The tension-extension curves of the SEC were seen to scale down in proportion to  $P_0$  at the stretched length. As the muscle was stretched there was an increase in the active muscle's compliance. According to the sliding filament hypothesis this was compatible with the instantaneous elasticity residing in the cross-bridges. The suggestion that the series compliance is a characteristic of the force developed leads to a new interpretation of the mechanism of cross-link activity.

Recently Huxley and Simmons (1971b) have proposed a new model to describe the mechanism of skeletal muscle contraction. Their scheme is based on the observations (see above) that the redevelopment of tension after a quick release (1 msec.) in a single muscle fiber occurs in two stages. The instantaneous drop in tension corresponding to the release is followed by a quick tension recovery and then a more gradual redevelopment. These authors proposed that a cross-bridge is attached to the myosin backbone by an undamped elastic element. On quick release there is an instantaneous change in length of this element. The tension-length curve obtained in this way resembles the characteristic tension-extension curve of the series elastic component. The external series compliance including the tendons has been eliminated by Huxley and Simmons with the use of their spot follower device which continuously measures the length of a middle segment of the fiber. It is further proposed that the head of the cross-bridge contains three sites  $M_1$ ,  $M_2$ ,  $M_3$ , each of which can combine with a



corresponding site ( $A_1, A_2, A_3$ ) on the actin molecule in the thin filament. The affinity between these sites is smallest for  $M_1, A_1$  and greater for  $M_2, A_2$  and so on. At any given time after stimulation two M sites are attached simultaneously to two A sites. The myosin sites are detached from the actin sites by a process involving the breakdown of ATP. At the peak of an isometric tetanus the greatest number of force producing links must be in their most stable position. Furthermore, the force is also present in the segment connecting the cross-link head to the myosin filament proper. A quick release produces an instantaneous drop in force of the undamped elasticity. The quick tension recovery is the result of the first attachment of M to A sites, as the myosin head rotates to a position of lower potential energy and thus stretches out the elastic element. Subsequent tension recovery is controlled by the rate constant for movement of the system from one stable position to the next. As new sites become attached, the myosin head is rotating and developing a force which is transmitted through the undamped elastic element to the myosin filament. It appears, therefore, that in an isometric contraction there is no need for the filaments to slide past each other to develop force. The elasticity of the cross-link allows it to rotate. However, in the isotonically contracting muscle sliding does occur.

If, as this model suggests, the cross-bridges are areas of relatively high compliance then the discrepancy between the observed and calculated myogram may be due to the erroneous conclusion that skeletal muscle contraction can be explained strictly in terms of Hill's two-component model.

### III. METHODS

The major part of this study deals with the instantaneous elasticity of contracting skeletal muscle, both at different lengths, and during the initial development of force in isometric tetani. It was also necessary to measure the mechanical  $a$  and  $b$  constants of Hill's characteristic equation in the toad muscle since reliable figures were not available in the literature. As well, mean sarcomere widths were measured using a light diffraction technique. Finally, the muscle's instantaneous elasticity during the decline of the active state has been studied.

All experiments to be reported here were carried out using sartorii of the toad Bufo bufo. The toad muscle has a convenient property that greatly recommends it for this work: over a large range of force the tension-extension curve of the SEC is approximately linear (Hill, 1970).

Definitions of frequently used terms are summarized in Table 1.

## 1. Elasticity Experiments

### a.) Materials

Pairs of sartorii were dissected with a small piece of pelvic bone attached. The body length ( $l_0$ ) of the muscle was determined by extending the legs and measuring the in situ distance from the pelvic bone to a piece of suture thread tied to the tibial tendon. Extreme care was taken to limit the length of tibial tendon (1 - 2 mm) remaining attached to the excised muscles. The muscles were then passed around a platinum wire stirrup, firmly connected to the anode pin of a RCA 5734 force transducer. The tibial tendons were tied with a small piece

TABLE I  
DEFINITIONS OF FREQUENTLY USED TERMS

$l_o$	-	length of the muscle measured in situ between the pelvic bone and a knot on the tibial tendon, with the legs extended.
$l_{max}$	-	length of the muscle at which the maximum isometric tetanic tension is obtained.
$P_o$	-	the maximum isometric tetanic tension at $l_{max}$ .
$(P_o)_l$	-	the maximum isometric tetanic tension at length $l$ .
Stiffness	-	gwt/mm; expressed throughout this thesis in terms of $P_o/l_o$ .
Compliance	-	mm/gwt.

of suture thread to a loop at the end of a straight annealed steel wire. The wire passed through a short brass tube and was connected to a metal rod which extended from the centre of a loud-speaker cone as shown in Fig. 3. In this way the muscles were held vertically in a bath of frog Ringer's solution (Adrian, 1956).

The movements of a vane on the metal rod were sensed by a focussed light-source-solar cell system ( $\Delta L$ , Fig. 3), the output from which was fed into the loud-speaker driver circuit. This feedback arrangement produced an extremely stiff and suitable fast length control system for examining the elastic properties of muscle. Further details of the length control system are given elsewhere (Clinch and Tennant, 1972). Figure 4 shows the closed-loop system's response to a ramp voltage input. It can be calculated that the initial acceleration of the system is in this case about 8g, comparing well with the figure given by Hill (1951b) of 4.5g for the Levin-Wyman ergometer accelerating to about the same final velocity (100 mm/sec). The smallest release duration which could be obtained without overshoot was about 2.5 msec. The stiffness of the closed loop loud-speaker system was measured as  $17 \times 10^3$  gwt/mm (about  $8500 P_o/l_o$ ); at least two orders of magnitude greater than the maximum values usually taken for the SEC (Hill, 1970). The overall stiffness of the system measured by connecting the metal rod from the speaker cone directly to the stirrup on the anode pin of the force transducer with a piece of annealed steel wire (analogous to the experimental conditions without the muscle) was  $966 P_o/l_o$ .

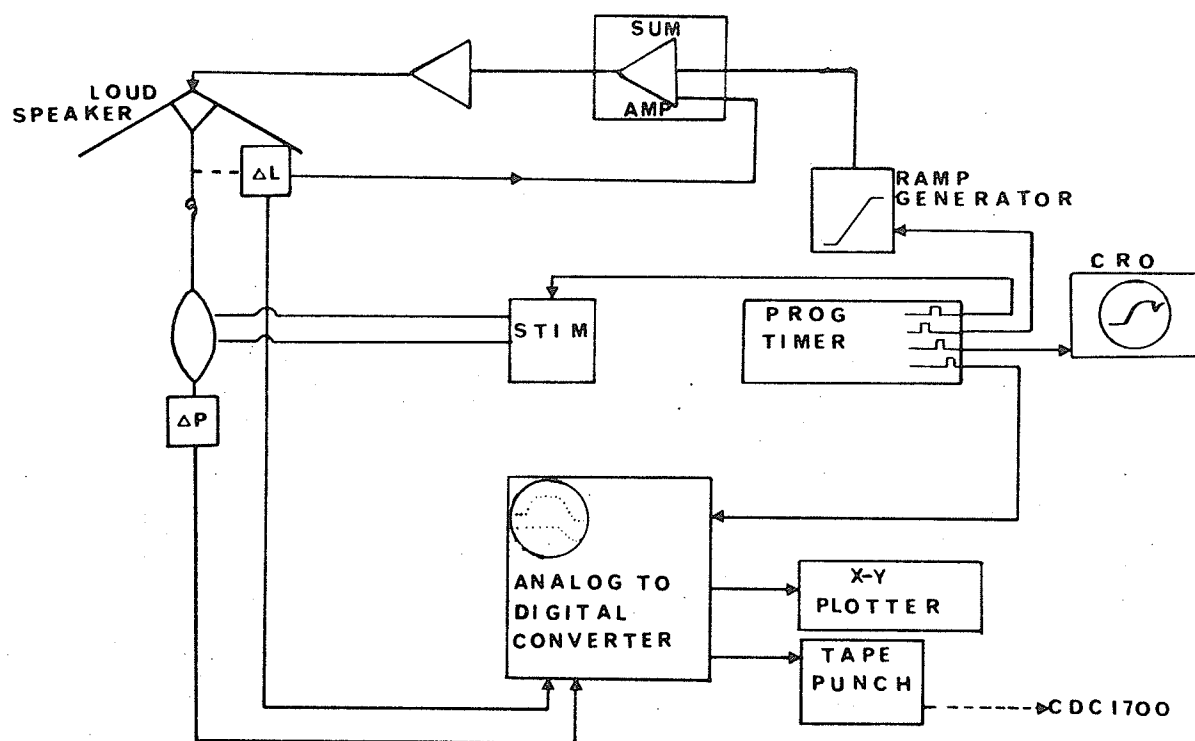


Figure 3: A block diagram of the apparatus. The length control loop is schematically shown by the length transducer ( $\Delta L$ ) and the two amplifiers at the top.  $\Delta P$  stands for the RCA 5734 force transducer. Other elements are described in the text.

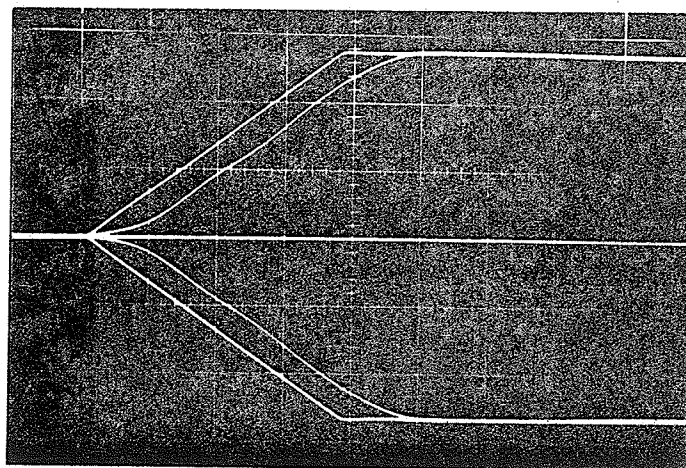


Figure 4: System response to ramp inputs, with time on the horizontal axis (1.0 msec/div.), input voltage and length output voltage on the vertical axis (0.2 volts/div.), which is equivalent to 0.14 mm/div. The centre horizontal line is zero length change. Upward deflections are stretches and downward deflections are releases of 0.38 mm at 105.6 mm/sec. In each case, the length change lags the input voltage.

This is approximately thirteen times the average maximum stiffness recorded in a large series of experiments with the toad muscles. A ramp generator, feeding into the speaker driver circuit was used to give linear stretches or releases of known rate and amplitude to muscles at different stages of contraction. A digital timer (Devices) triggered a stimulator (Devices), oscilloscope (Tektronix, 565), computer of average transients (CAT 400C, Technical Instruments Inc.) and the ramp generator (Exact), at preset times during a contraction cycle (Fig. 3).

b.) Experimental Procedure

The muscles were set up at  $l_{\max}$ , the length at which the biggest tetanus was obtained. They were then stimulated at regular intervals until a steady state was revealed. This stimulus pattern consisted of a single twitch or brief tetanus every 99 seconds for an initial 2 hour period. During the experiment, the same time sequence was maintained with every two twitches followed by a 750 msec tetanus (stimulus frequency 11 - 15 shocks/sec). All-over transverse stimulation of the muscles was achieved by means of supra-maximal, 1 msec square pulses given via two multi-electrode arrays, one on each side of the pair of muscles and parallel to, but not touching, their flat faces. The Ringer solution was bubbled with oxygen and kept at less than  $1^{\circ}\text{C}$  by means of a large stirred ice bath. The temperature of the Ringer solution was measured with a calibrated thermistor probe lying close to the muscles.

Force-extension curves were obtained by giving the muscle a constant



velocity release from the plateau of an isometric tetanus, a method first used by Hill (1950a) or at various times during the initial development of force (Clinch and Bressler, 1971). The analog outputs from the length and force transducers were digitised in the CAT at a rate of 0.625 msec/address and written out onto punched paper tape for further analysis.

In addition, some experiments were done by the quick release method. For this method the release was made too small to reduce the force to zero and one simply notes the minimum in the force record corresponding to the end of the release. From a series of such releases (small stretches can also be used) a graph is constructed relating minimum (or maximum) force to the extent of the release (or stretch). The same correction for internal shortening and the same qualifications about release speed apply here as in the controlled release experiments. The results from both types of experiments were similar but the controlled release method was preferred as it limits the amount of time the muscle is stimulated. With this technique a single release to zero tension produced a complete tension-extension curve whereas only one point at a time was obtained with each quick release.

### c.) Analysis of Data

Force values were normalized with respect to maximum tetanic force ( $P_0$ ) and the changes in length were normalized with respect to body length ( $l_0$ ). Plotting force against the change in length produces a tension-extension curve. The linearity of this curve permitted us to do linear regression analysis of the

points from  $0.4 P_0$  to  $P_0$  and use the slope of the line as a measure of the instantaneous stiffness of the muscle. The tension-extension curves were not corrected for the compliance of the transducer and connections. The regression analysis gave a value for the square of the correlation coefficient which was never below .990, confirming the linearity of the force-extension curve over the range of force values considered.

#### d.) Active State and Instantaneous Elasticity

The decay of the active state was measured in three pairs of toad sartorii by giving a single release to about  $0.5 P_0$  at various times during an isometric tetanus (Ritchie, 1954). The maximum redeveloped tension  $P$  and the time  $t$  at which it occurs are plotted and represent the intensity of the active state at times after  $P_0$  is reached. The release records were simultaneously digitised in the CAT and tension-extension curves obtained as already described.

## 2. Force-Velocity Experiments

In order to correct for any internal shortening of the contractile component during the releases it became necessary to determine the force-velocity curve for the toad sartorius. Pairs of sartorii were placed on a multielectrode assembly and connected from their tibial tendons with a jeweller's chain to a conventional isotonic lever (Fig. 5). Tension was recorded from the pelvic end of the muscles as described above. The moving core of a Hewlett Packard variable inductance length transducer, mounted near the fulcrum of the lever, was used to measure the shortening against different loads. The output of the

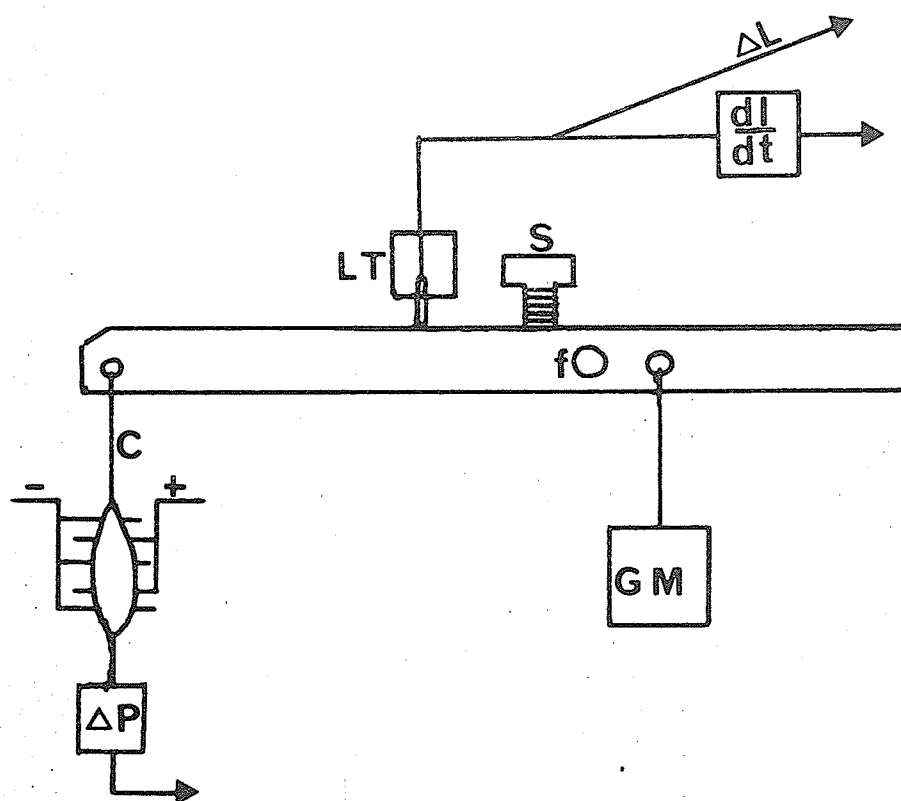


Figure 5: Experimental set up for force-velocity experiments. The usual set up is used to measure tension and for stimulating. The tibial (upper) end of the muscle is connected via a light jeweller's chain, C, to a conventional isotonic lever. LT is the length transducer, S is the after-load stop, f is the fulcrum of the lever,  $\Delta P$  is a RCA 5734 force transducer. The load (GM) on the lever is hung close to f to reduce inertia effects to a negligible level. The tension, length, and velocity changes are recorded.

length transducer could be differentiated electronically and both tension, length, and velocity changes were displayed on a two gun oscilloscope, and recorded on film. In some of the experiments the length and tension signals were fed into the CAT and written out on an X-Y plotter.

Force-velocity curves were also determined by giving the muscle a constant velocity release at different times during an isometric tetanus and noting the steady tension reached (Hill, 1970). In Figure 6 is seen an example of a controlled velocity release of  $.5 l_o/sec$  given at 55 msec after the first shock, resulting in a steady tension level of  $.2 P_o$ . The middle trace is the same release given at 80 msec. In this instance the release is initially too fast resulting in a fall in tension. However, when the speed of release is the same as the velocity of shortening of the contractile component, the same tension level of  $.2 P_o$  is maintained. Similarly, if the release comes too early in the contraction, i.e. is initially too slow, the muscle will continue to develop force and eventually reach a steady tension, shortening at a velocity equal to the speed of the release. The uppermost trace in Figure 6 is a short tetanus which does not reach  $P_o$ .

### 3. Diffraction Patterns of Toad Sartorii

A 2 mw helium-neon gas laser was used to obtain diffraction patterns of the toad (Bufo bufo) sartorius. The muscle was dissected and placed on a multi-electrode stimulating assembly that was housed in a perspex chamber filled with Ringer's solution. The temperature of the bath was maintained at about  $10^{\circ}C$ .

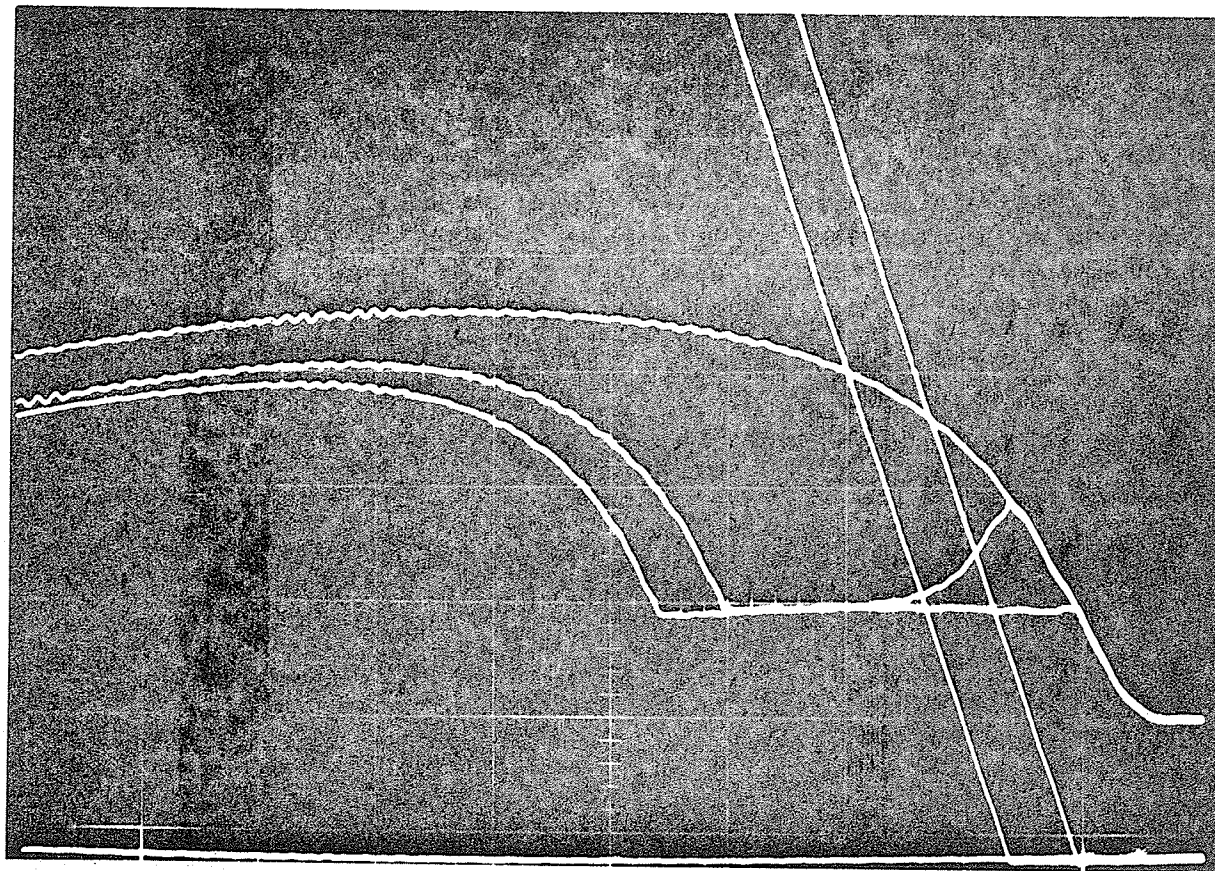


Figure 6: A record from a controlled-velocity-release experiment. Time on horizontal axis ( 50 msec/div.), length on vertical axis (210  $\mu$ /div.), and tension on vertical axis (7.7 g/div.). The bottom trace is the tension during a release of .5  $l_0$ /sec given at 55 msec. The middle record is a release of the same velocity given at 80 msec. The top trace is a short isometric tetanus at 0°C. The corresponding length records are also shown. Toad sartorius,  $l_0 = 22$  mm., wt. = 63 mg.

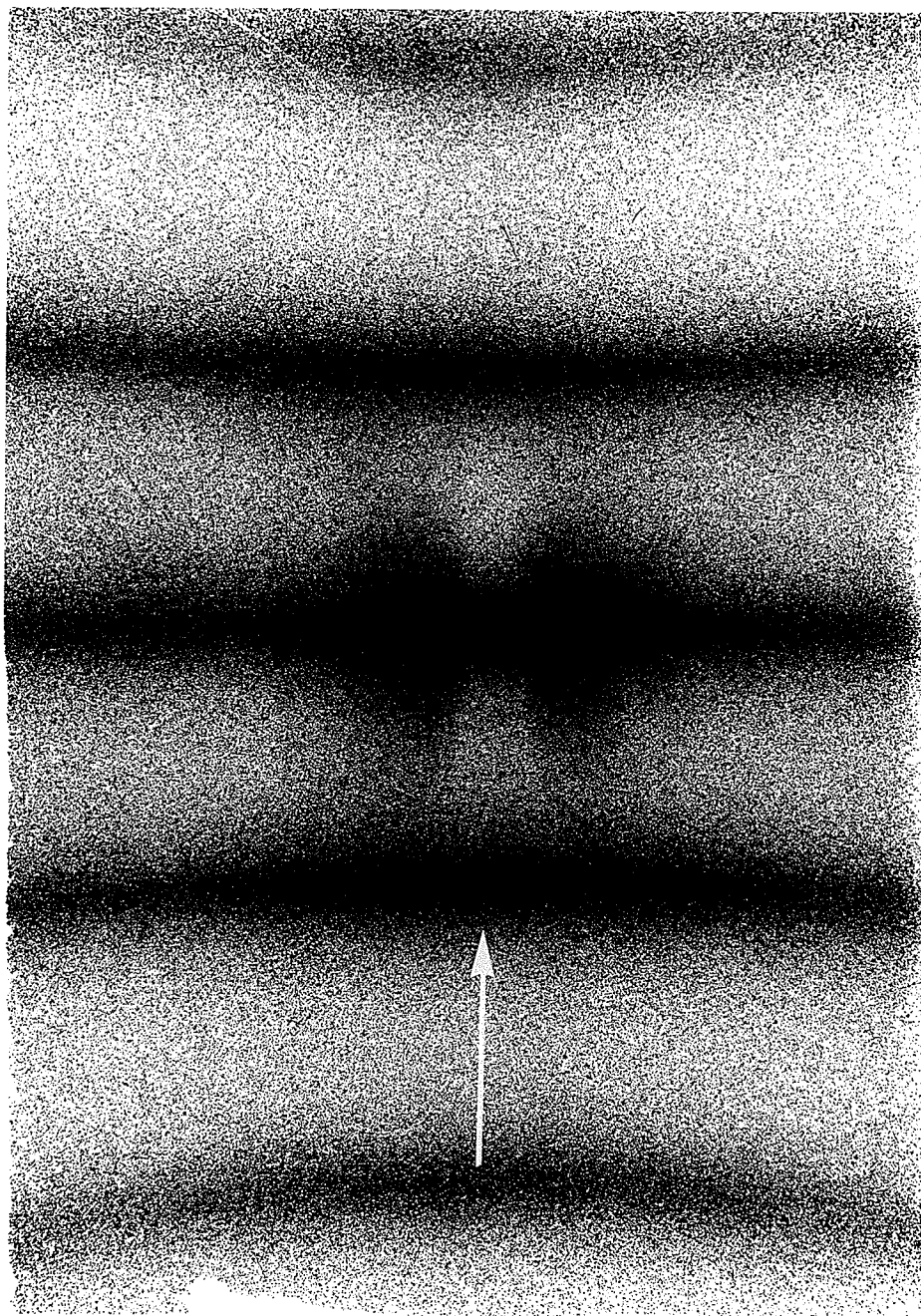


Figure 7: The diffraction pattern from a toad sartorius at  $l_0$  showing zero (center), first, and second order bands. The distance between the center of the first order bands ( $2d$ ) was measured with a densitometer. Measurements were made close to the midline (arrow) to avoid possible distortion effects near the periphery of the photograph. Calculated sarcomere spacing in this instance with  $d = 16.35 \text{ mm}$  is  $2.51 \mu$ .

The pelvic bone of the muscle was clamped firmly in place at the bottom of the chamber, while the tibial tendon was connected vertically with a short piece of jeweller's chain to the anode pin of a RCA 5734 force transducer. The force transducer was mounted on a micromanipulator and could be raised or lowered to adjust the length of the muscle.

The muscle chamber assembly, epoxied to a brass rod, was attached to a heavy Harvard screw stand which was used to bring the muscle in line with the laser beam. The laser was mounted securely on a heavy piece of brass plate. A Bower X bellows camera, with all the lenses removed, was placed on the face of the laser. This permitted exposures of varying duration by adjusting the shutter speed of the camera. The light beam entered and left the muscle chamber by way of two windows made of Corning glass coverslips. The stimulating apparatus contained a hole through which the laser beam passed. Film holders (dark slides) containing Kodak Pan 4155 sheet film were placed a fixed distance from the muscle chamber.

The body length of the muscle was measured in situ and then set up at this length in the chamber. After a short equilibration period the length at which the muscle gave the biggest isometric twitch was determined using single supramaximal shocks. Diffraction patterns were then recorded at various lengths. At short lengths, the muscle was given a couple of shocks to take up the slack.

Figure 7 is a photograph of the diffraction pattern of a muscle at  $l_0$ . The fringe width between the bands,  $d$ , was measured from the film with a

densitometer. This distance was then used in the following equation:

$$\bar{S} = \frac{n \lambda}{\sin(\tan^{-1} \frac{d}{D})} \quad (1)$$

where  $D$  is the distance from the muscle to the film,  $d$  is the measured distance between the bands,  $n$  is the order of the bands (usually equal to 1),  $\lambda$  is the wavelength of the light in vacuo (.633  $\mu$ ), and  $\bar{S}$  is the calculated width of the sarcomere. Equation (1) is not sufficient however if the chamber contains Ringer's solution, since the wavelength decreases when light enters a medium of high refractive index according to the relation:

$$\mu = \frac{\lambda_o}{\lambda_m}$$

where  $\lambda_o$ ,  $\lambda_m$  are wavelengths of the light in vacuo and in Ringer's solution respectively, and  $\mu$  is the refractive index of Ringer's solution (taken as equal to  $\mu$  for pure water, 1.33). Furthermore, the diffracted rays are bent away from the normal as they pass from the chamber into the surrounding air according to Snell's law:

$$\mu_{WA} = \frac{\sin \Theta_A}{\sin \Theta_W}$$

where  $\Theta_A$  is the angle between the normal and the ray in air, and  $\Theta_W$  is the angle between the normal and the ray in water (in this case Ringer's solution) and  $\mu_{WA}$  is the index of refraction of water with respect to air. Small errors in the estimation of  $\bar{S}$  caused by these two effects could be corrected by using



the modified equation:

$$d = \frac{B (.633/\bar{S})}{(1 - (.633/\bar{S})^2)^{1/2}} + \frac{10 (.633/(1.33 \times \bar{S}))}{(1 - (.633/(1.33 \times \bar{S}))^2)^{1/2}}$$

This equation was routinely used in calculation of the sarcomere lengths.

#### IV. RESULTS

## 1. Force-Velocity Experiments

Hill (1949) gives values of the constants  $a$  and  $b$  in a single experiment with toad sartorii at  $0^{\circ}\text{C}$  as  $0.21 P_0$  and  $0.21$  lengths/sec respectively, but unfortunately the body length of this muscle is not recorded. The pooled data from twelve force-velocity experiments, summarized in Table II, is shown in Figure 8. No consistent difference is apparent between curves obtained with a conventional isotonic lever technique (open circles) or with constant velocity controlled releases at different times during isometric force development (filled circles), although Hill (1970) has described such differences in frog sartorii, and Parmley, Yeatman and Sonnenblick (1970) have described it for cat papillary muscle, rat soleus, and strips of heart muscle from *Limulus polyphemus*. The means and standard error of the means of the normalized constants from 12 experiments were:

$$a/P_0 = 0.22 \pm .01$$

$$b/l_0 = 0.28 \pm .01$$

The temperature of the bathing solution in each case was measured as less than  $1^{\circ}\text{C}$ .

## 2. Elasticity Experiments

A typical CAT record is shown in the inset of Fig. 9. The CAT sweep was triggered 50 msec before the start of the release (725 msec after the first shock of the tetanus). The first 25 msec of the tension trace (not shown) is short circuited to provide a baseline, followed by peak tetanic tension and the release.

TABLE II

VALUES OF THE FORCE-VELOCITY CONSTANTS FOR THE TOAD SARTORIUS  
FROM ISOTONIC AND CONTROLLED VELOCITY RELEASE EXPERIMENTS

Date	Isotonic Experiment	Controlled Velocity Release Experiment	$a/P_o$	$b/l_o$	$V_{\max}$ $l_o/\text{sec}$
14. ix. 71	+		.20	.22	1.10
14. ix. 71		+	.24	.34	1.42
16. ix. 71	+		.19	.22	1.16
16. ix. 71		+	.27	.35	1.30
17. ix. 71	+		.21	.27	1.29
17. ix. 71		+	.16	.23	1.44
20. ix. 71	+		.26	.35	1.35
20. ix. 71		+	.24	.30	1.25
23. ix. 71	+		.19	.35	1.84
23. ix. 71		+	.24	.35	1.46
4. x. 71		+	.21	.21	1.00
13. x. 71		+	.18	.22	1.22

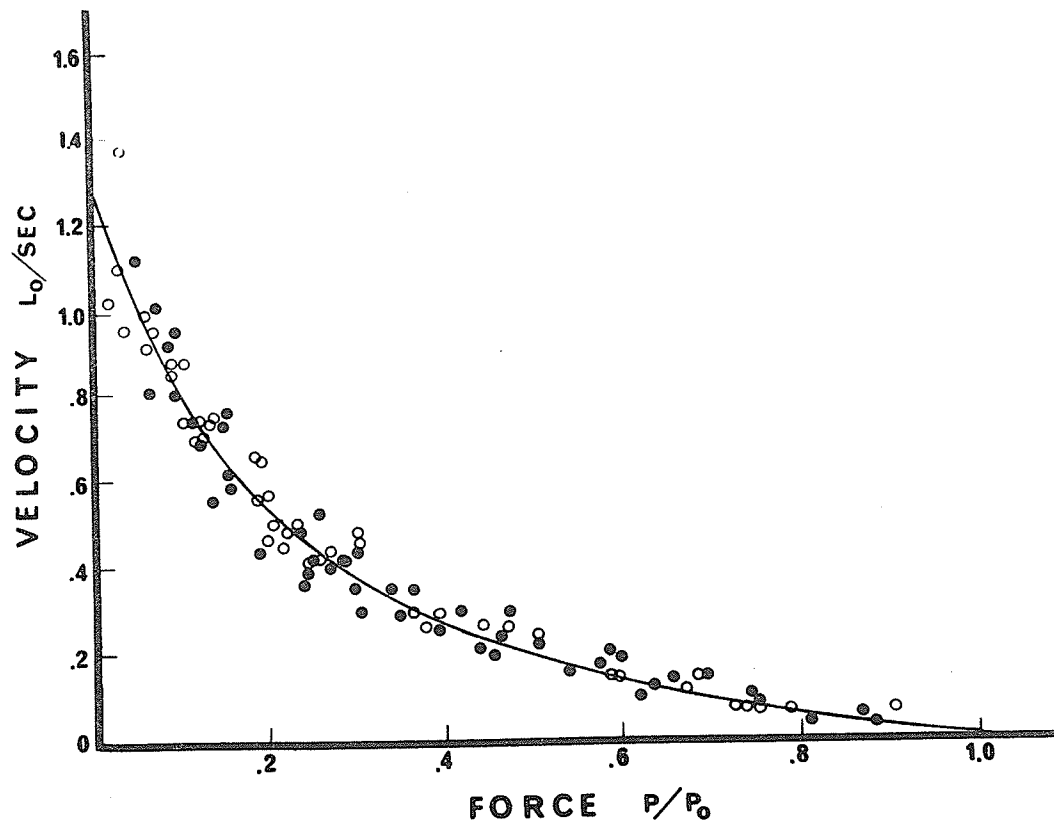


Figure 8: A graph showing the distribution of force-velocity points from twelve separate experiments on toad sartorii. Open circles represent values obtained with a conventional isotonic lever. Closed circles represent values obtained by controlled releases. The line drawn is calculated using Hill's equation with values of  $a/P_0 = .22$  and  $b = .28 \text{ } l_0/\text{sec}$ .

The velocity of the length change in this particular record was  $2.3 \text{ l}_0/\text{sec}$ . The tension-extension curve derived from this record and shown in Fig. 9, is representative of the curves obtained during the course of these experiments. The regression line through the points from  $0.4 P_0$  to  $P_0$  gives a correlation coefficient squared of .996 and a stiffness value of  $60 P_0/l_0$ . In twenty separate experiments the average stiffness at  $P_0$  for toad sartorii was found to be  $75 P_0/l_0 (\pm 3.86 P_0/l_0, \text{S.E. of the mean; see Table III})$ .

#### a.) Active State and Instantaneous Elasticity

In order to rule out possible changes in the instantaneous stiffness of a contracting muscle shortly after the last shock of a tetanus, experiments were undertaken to compare it with the decline of the active state. Figure 10 shows the decay of the active state in a single toad sartorius compared with the fall in tension from the peak of an isometric tetanus and the instantaneous stiffness of the same muscle at various times after the last shock. The duration of the active state was 115 msec corresponding to a duration of 90 msec reported by Hill (1953a) for the frog sartorius at  $0^\circ\text{C}$ . The tension starts to fall at 200 msec while the muscle's stiffness stays close to maximum for approximately 625 msec after the last shock. The beginning of the decline in stiffness coincides with a tension of  $.85 P_0$ . The stiffness stays at the maximum measured at  $P_0$  for a considerable time while the active state is decaying. This permits some flexibility in the time after the last shock at which the tension-extension curve is obtained. Our stiffness measurements were routinely made at 50 msec after the last shock, which

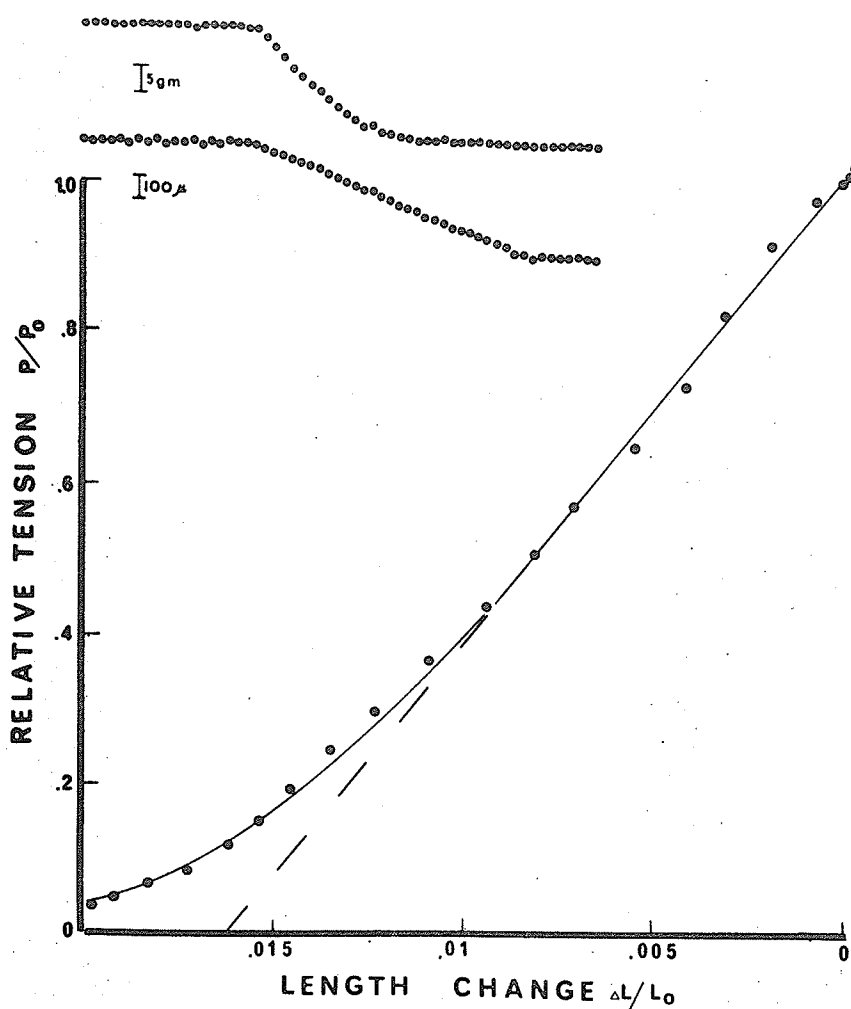


Figure 9: Tension-extension curve from  $P_0$  in a contracting muscle. Abscissa: length change normalized with respect to body length. Ordinate: tension normalized with respect to maximum tetanic tension at  $l_0$ . The regression line through the points from  $0.4 P_0$  to  $P_0$  gives a measured stiffness of  $60 P_0/l_0$ . The inset at the top of the figure shows the original record of the release as produced by the computer of average transients. The upper trace represents tension, the lower one length. The time interval of analysis is 0.625 msec/address and the 5 gwt force calibration bar corresponds to a counts/address change of 10.6 counts. Toad sartorius,  $0^\circ\text{C}$ ,  $l_0 = 24 \text{ mm.}$ , wet wt. = 64 mg.,  $P_0/l_0/m = 1125 \text{ g/cm}^2$ .

TABLE III

STIFFNESS VALUES FOR THE TOAD SARTORIUS AT

 $l_{\max}$ 

Date	Stiffness $P_o/l_o$
9. iii. 71	50
15. iii. 71	74
13. v. 71	73
15. v. 71	80
15. v. 71	79
11. ix. 71	65
27. ix. 71	70
4. x. 71	55
13. x. 71	55
26. x. 71	65
1. xi. 71	61
24. xi. 71	85
2. xii. 71	61
13. xii. 71	66
4. iv. 72	81
5. iv. 72	80
2. v. 72	111
3. v. 72	101
5. v. 72	92
6. v. 72	108



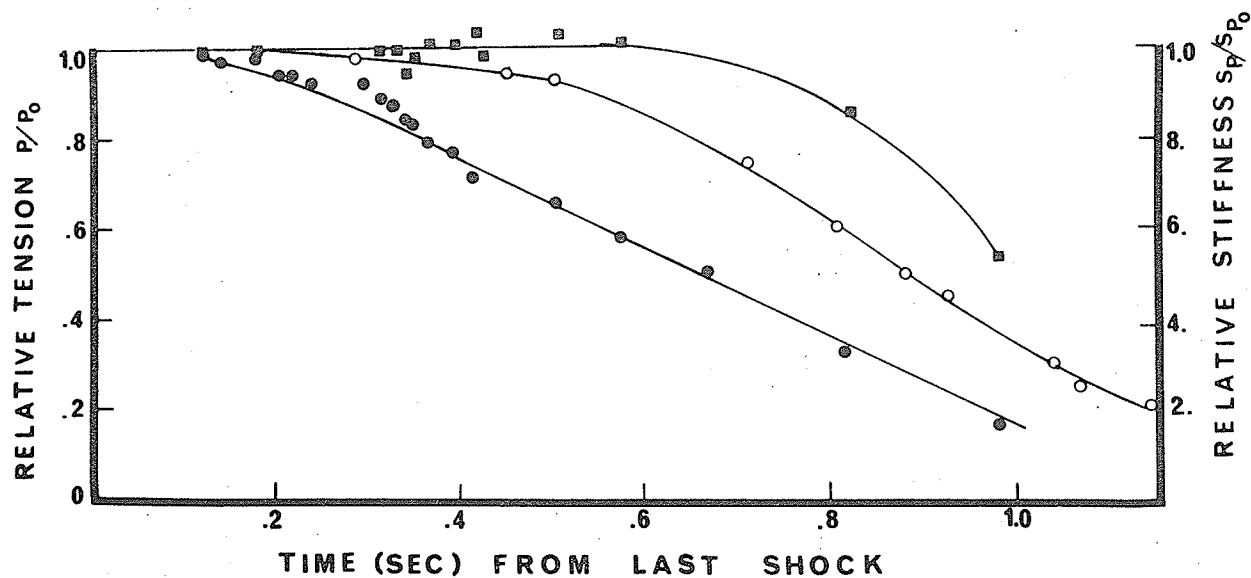


Figure 10: The decay of the active state in an isometric tetanus compared with the fall in tension from  $P_0$  and the instantaneous stiffness at different times after the last shock. ●, the decline of the active state; ○, the fall in tension from  $P_0$ ; ■, the instantaneous stiffness. Both tension and stiffness values are expressed as fraction of their maximum values at  $l_0$ . Toad sartorius at  $0^\circ\text{C}$ ,  $l_0 = 24.5$  mm, wt. = 53 mg.

provided a sufficient number of points during maximum tetanic tension for accurate computation of  $P_o$ .

b.) Velocity of Release

To what extent does the measured stiffness of the muscle depend on the speed of the release? Figure 11a shows tension-extension curves from the peak of an isometric tetanus obtained with release speeds of  $4.75 \text{ l}_o/\text{sec}$  (101 mm/sec),  $2.54 \text{ l}_o/\text{sec}$  (56 mm/sec) and  $.73 \text{ l}_o/\text{sec}$  (16 mm/sec). The slowest release gives points which diverge markedly from the others at low tensions. Of course in terms of the two component model this is to be expected: at low speeds a significant fraction of the release will be taken up by the shortening of the contractile component. A test of the two component theory is to calculate the amount of this "internal shortening" and to subtract it from the imposed length change during releases at different speeds. This calculation should bring the curves of Figure 11a together if the two component model is a good approximation to the muscle's behaviour. In order to carry out the correction it is only necessary to know the force-velocity curve of the tetanized muscle at body length. This was determined and the correction for internal shortening was done by calculating the mean shortening between two points from the mean force, using Hill's characteristic equation in the form:

$$V = \frac{(P_o - P)b}{P + a}$$

where  $V$  is expressed in units of  $\text{l}_o/\text{sec}$ , given values of  $P$  expressed at  $P/P_o$ .

The analysis interval corresponded to the inter-address time of 0.625 msec. In

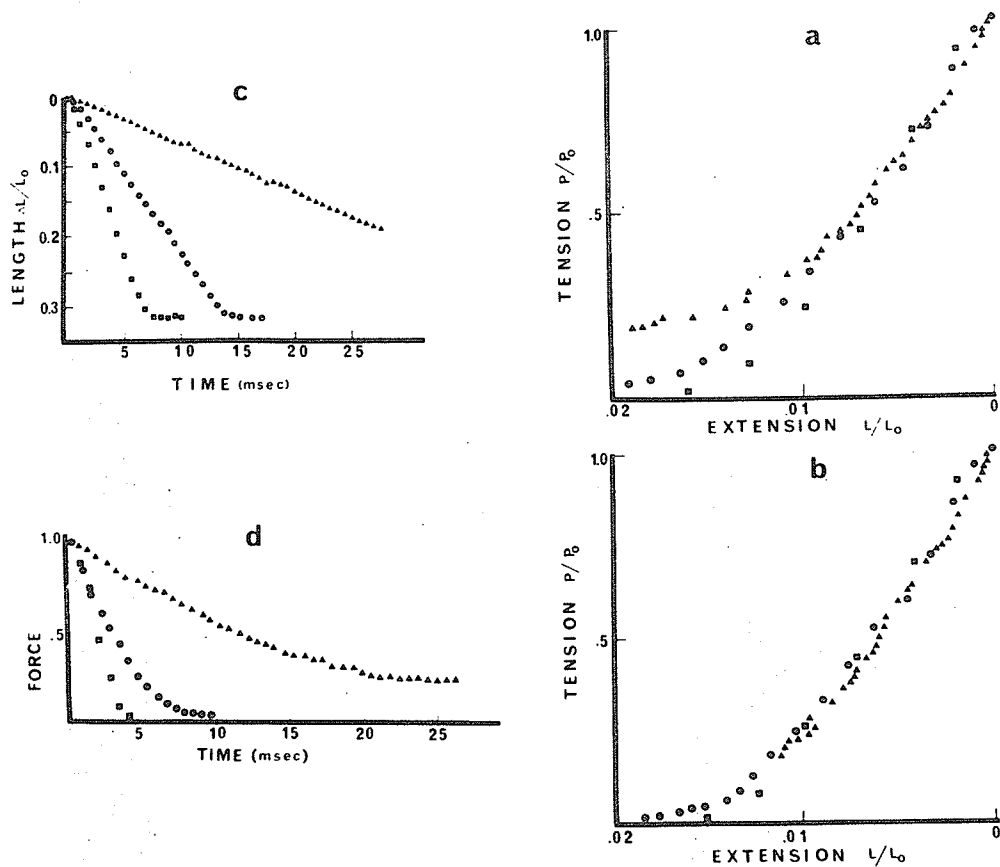


Figure 11: (a) Three tension-extension curves from the same pair of muscles, obtained from peak tetanic tension with release velocities of:  $\Delta = .73 l_0/\text{sec}$ ,  $\bullet = 2.5 l_0/\text{sec}$ ,  $\blacksquare = 4.5 l_0/\text{sec}$ . Toad sartorius at  $0^\circ\text{C}$ ,  $l_0 = 22 \text{ mm}$ .

(b) The same three curves as in (a) but corrected for internal shortening of the contractile component.

(c) The change in length with time after the start of the release, at the velocities indicated in (a). The release durations are:  $\Delta = 27.5 \text{ msec}$ ,  $\bullet = 15.6 \text{ msec}$ ,  $\blacksquare = 8.1 \text{ msec}$ .

(d) The change in force with time after the start of the release, at the velocities indicated in (a).

Figure 11b we see that the correction succeeds in bringing the curves together. The apparent non-linearity in the original length and tension records (Fig. 11c, Fig. 11d) are due to the quantization error of the computer of average transients. The quantization error represents the smallest fractional change in the incoming analog signal that can be digitized by the computer, which for these records was a 3% change.

Similar results were obtained in a number of other experiments involving releases from  $P_0$ , and in one case, from a point midway on the isometric myogram 75 msec after the beginning of stimulation. This correction for internal shortening has therefore been used in all our analyses. The major effect of the correction is to bring the curves of Fig. 11a together in the region of low force. In the high force region the curves are not much affected. Over the range of our measurements there seems to be very little effect of speed of release on the muscle's stiffness, in agreement with Hill (1953b). A similar finding for single fibers and bundles of fibers from frog semitendinosi has been reported by Civan and Podolsky (1966).

The upper limit to the useful release velocity was set by two factors: the number of points on the tension-extension curve necessarily fell as the release velocity increased, and at high speeds (release time  $< 5$  msec) there appeared a delay of about 1 msec between the onset of the length change and the beginning of the tension drop. This could perhaps be accounted for in terms of the time taken for propagation of the displacement pulse through the muscles from their tibial ends to the force transducer at the pelvic end. This time may be estimated

from the standard formula for the rate of propagation of a longitudinal wave along a rigid rod:

$$t = \frac{l}{(E_Y/\rho)^{1/2}}$$

where  $t$  is the propagation time over a distance  $l$  (taken as 2.5 cm),  $E_Y$  is Young's Modulus (taken from our results as  $1.5 \times 10^3$  N/cm<sup>2</sup>) and  $\rho$  is the muscle density (1 g/cm<sup>3</sup>). Calculated in this way,  $t$  is found to be 0.2 msec, but it is not clear to what extent the muscle can be treated as a rigid rod although a similar assumption has been made by Blangé, Karemaker, and Kramer (1972). When the muscle is replaced with a suitable spring of known compliance a similar delay in tension drop can be calculated which is the same as the observed delay. The release velocity finally used was between 1.4 and 2.5  $l_0$ /sec; in the range where a large correction factor for internal shortening was unnecessary and no problems arose due to the excessive speed of release. The time taken for tension to fall to zero at these release speeds was about 10 msec.

### c.) Tension-Extension Curves at Long Lengths

In Fig. 12 are three tension-extension curves obtained by the method of quick stretches and releases, in the same muscle at different lengths. A decrease in muscle stiffness is shown by a decrease in the slope of the line through the points as is evident in the 1.2  $l_0$  and 1.3  $l_0$  curves. The stiffness values obtained for these curves are 74  $P_0/l_0$  ( $l_0$  curve), 54  $P_0/l_0$  (1.2  $l_0$  curve) and 50  $P_0/l_0$

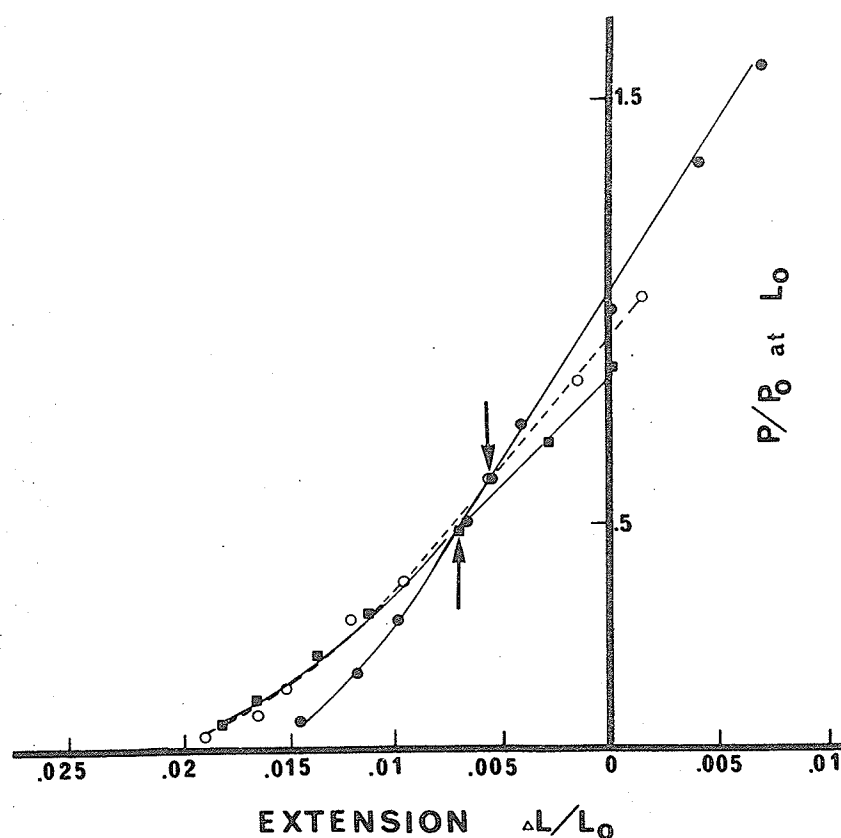


Figure 12: Tension-extension curves from maximum tetanic tension of a contracting muscle at three different lengths,  $\bullet = l_0$ ,  $\circ = 1.2 l_0$ ,  $\blacksquare = 1.3 l_0$ . Abscissa: length change as a fraction of body length. Ordinate: tension at different lengths normalized with respect to maximum tetanic tension at  $l_0$ . The arrows indicate the points at which the curves are made to fit. The curves at long lengths are shifted horizontally so that the point  $(P_0)_l$  lies on the  $l_0$  curve. Method used to obtain these curves was quick stretches (positive  $\Delta l$ ) and releases (negative  $\Delta l$ ). Toad sartorius,  $0^\circ\text{C}$ ,  $l_0 = 23\text{ mm}$ .

(1.3  $l_0$  curve). To facilitate comparison, the curves at long lengths are shifted horizontally so that the point  $(P_0)_1$  lies on the  $l_0$  curve. The reason for this can be seen by imagining the elasticity of the muscle to be limited by some inert, constant component such as the tendons or the compliance of the recording equipment. This method of plotting the curves obtained at different lengths would then cause them to superimpose since they would essentially be segments of the same curve. Figure 12 shows that this is clearly not so; the compliance of a muscle as a function of load is not the same at different lengths but increases as the overall muscle length increases. This is not predicted by Hill's formulation of the two component model, but is to be expected if a large part of the compliance of active muscle resides in the sarcomeres. To investigate this possibility more closely we examined the relationship between the maximum stiffness at any given length and the maximum developed isometric tension at that length. At lengths above 1.1  $l_0$  a correction had to be made for the contribution of the parallel elastic component to the measurable stiffness of the unstimulated muscle. The procedure adopted was to subtract a record of release of the unstimulated muscle from a record of an identical release of the actively contracting muscle (Jewell and Wilkie, 1958). The stiffness and tension values at long lengths for 9 separate muscles is summarized in Table 4. A statistical comparison of these values using a two sample t-test for populations with equal variances indicated that the small difference observed between the means (Fig. 13) was in no case significant ( $P > .3$  in the 1.3  $l_0$  points). The relation between the

TABLE IV

STIFFNESS AND TENSION VALUES FOR THE TOAD SARTORIUS AT LONG LENGTHS

Date	Length $l/l_o$	*Relative Tension $(P_o)/P_o$	Stiffness $(P_o)/l_o$	Stiffness $P_o/l_o$	*Relative Stiffness $S_l/S_l_o$
9.iii.71	1.0	1.0	50	50	1.0
	1.2	.71	61	43	.80
	1.3	.36	72	26	.51
15.iii.71	1.0	1.0	74	74	1.0
	1.2	.61	89	54	.73
	1.3	.49	102	50	.54
13.v.71	1.0	1.0	73	73	1.0
	1.1	.85	78	67	.92
	1.2	.76	75	57	.79
15.v.71	1.0	1.0	80	80	1.0
	1.1	.98	74	72	.91
	1.2	.36	77	66	.83
	1.3	.64	79	50	.63



TABLE IV (continued)

Date	Length $l/l_o$	* Relative Tension $(P_o)/P_o$	Stiffness $(P_o)/l_o$	Stiffness $P_o/l_o$	* Relative Stiffness $S_l/S_{l_o}$
15. v. 71	1.0	1.0	81	81	1.0
	1.1	.95	79	75	.95
	1.2	.75	84	63	.80
4. x. 71	1.0	1.0	55	55	1.0
	1.2	.77	57	44	.80
	1.3	.57	57	32	.59
26. x. 71	1.0	1.0	65	65	1.0
	1.2	.84	64	54	.83
	1.3	.64	75	48	.74
1. xi. 71	1.0	1.0	61	61	1.0
	1.1	.90	57	51	.84
	1.2	.80	61	49	.80
	1.3	.56	65	42	.69

TABLE IV (continued)

Date	Length $l/l_o$	*Relative Tension $(P_o)l/P_o$	Stiffness $(P_o)l/l_o$	Stiffness $P_o/l_o$	*Relative Stiffness $S_l/S_l_o$
2.xii.71	1.0	1.0	61	61	1.0
	1.1	.84	61	51	.84
	1.2	.71	61	44	.71

\*No significant difference was seen between the values in these columns.

$P > .7$  1.1  $l_o$  points

$P > .3$  1.2  $l_o$  points

$P > .3$  1.3  $l_o$  points

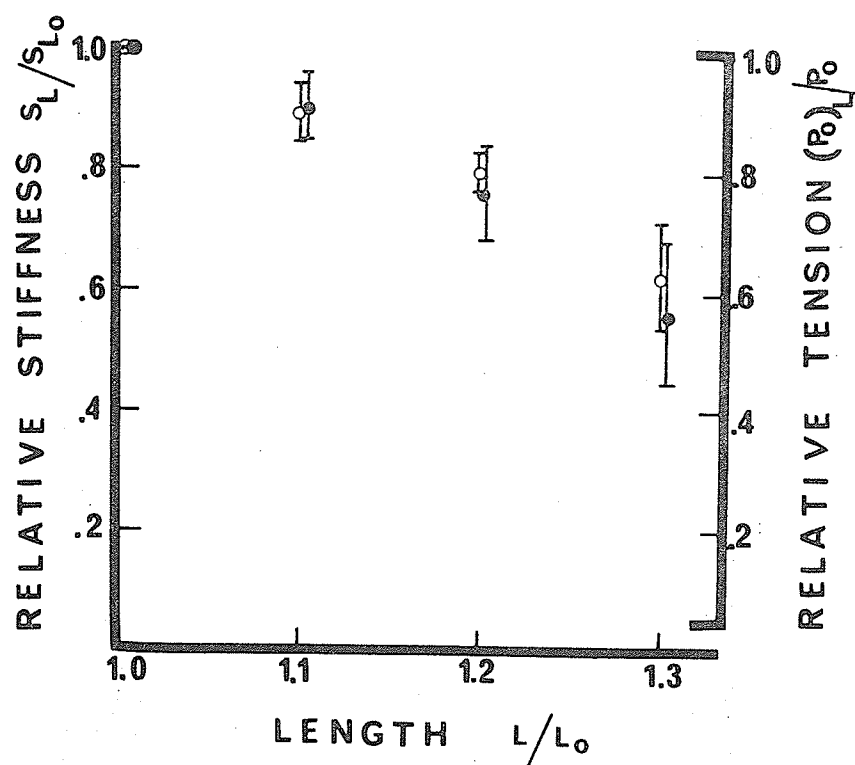


Figure 13: Mean values for the maximum stiffness ( O ) and maximum tetanic tension ( ● ) for toad sartorii at long lengths (see Table IV). The bars represent the standard deviation of a single observation. Both stiffness and tension are normalized with respect to their maximum values at body length.

maximum stiffness and the maximum tetanic force, at a given length, ( $l > l_0$ ) is shown in Fig. 14. The correlation coefficient for these points is  $r = .95$ . The positive correlation between the stiffness of the contracting muscle and the developed force strongly suggests that the force generating elements within the muscle may be sites of relatively high compliance.

d.) Tension-Extension Curves at Short Lengths

Distinctly different predictions are made about the stiffness-length and stiffness-force curves, at  $l < l_0$ , if the series compliance resides entirely in the unbonded I-filaments or if the cross-bridges are the major source of compliance in an active muscle. If all the stiffness were in the unbonded I-filaments then at short lengths a large increase in muscle stiffness would be predicted as there was less unbonded thin filament in series with the contractile machinery (see Appendix 1). For this reason the instantaneous elasticity of a contracting muscle at lengths below  $l_0$  has been measured (Table V). Figure 15 shows four tension-extension curves from the same muscle at short lengths. The stiffness values obtained for these curves are  $77 P_0/l_0$  ( $l_0$  curve),  $63 P_0/l_0$  ( $.8 l_0$  curve),  $50 P_0/l_0$  ( $.72 l_0$  curve) and  $37 P_0/l_0$  ( $.68 l_0$  curve). The compliance of the muscle is decreasing as the overall muscle length decreases. Furthermore, as was seen in the experiments at long lengths, if these curves were shifted along the horizontal axis so that the point  $(P_0)_l$  lies on the  $l_0$  curve they would not be part of the same curve, indicating once again that the compliance of a muscle as a function of load is not constant at different lengths. The relationship between

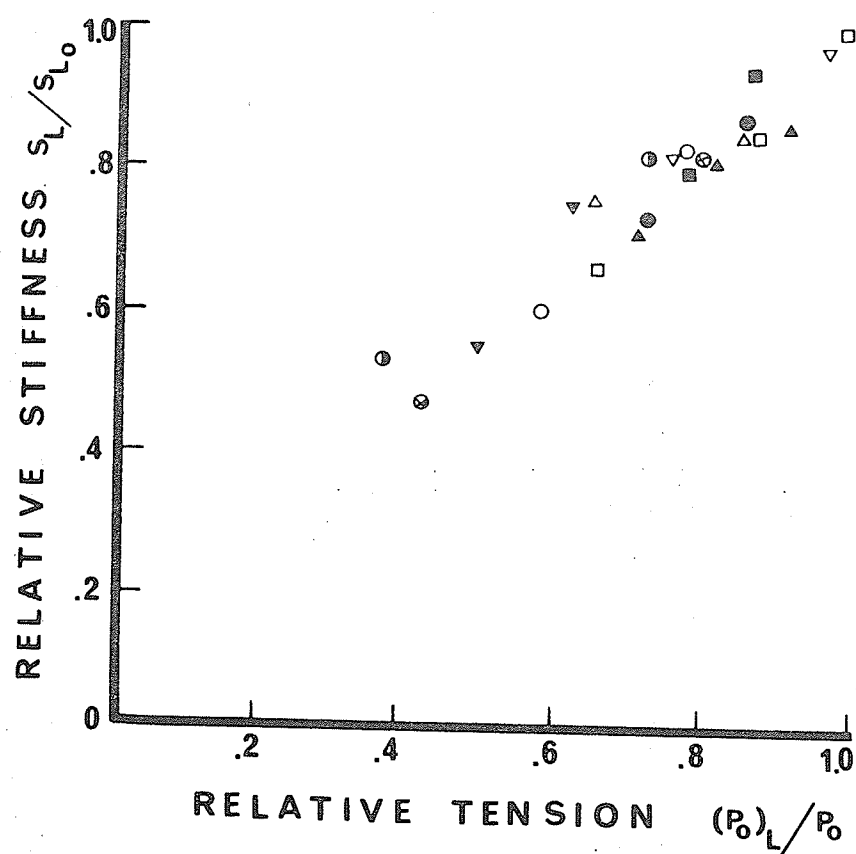


Figure 14: The relation between maximum stiffness and tetanic force in toad sartorii at long lengths. The different symbols refer to the results of nine experiments and both stiffness and tetanic force are expressed as fractions of their respective values at body length.

TABLE V

## STIFFNESS AND TENSION VALUES FOR THE TOAD SARTORIUS AT SHORT LENGTHS

Date	Length $l/l_o$	Relative Tension $(P_o)/P_o$	Stiffness $(P_o)/l_o$	Stiffness $P_o/l_o$	Relative Stiffness $S_l/S_{l_o}$
4. iv. 72	1.0	1.0	81	81	1.0
	.79	.72	107	77	.95
	.71	.50	132	66	.82
5. iv. 72	1.0	1.0	77	77	1.0
	.88	.87	88	76	.99
	.80	.62	102	63	.82
	.72	.33	148	50	.64
	.68	.21	174	37	.48
2. v. 72	1.0	1.0	111	111	1.0
	.93	1.0	108	109	.99
	.90	.98	110	108	.98
	.82	.87	129	112	1.01
	.79	.74	134	100	.90
	.75	.62	163	102	.92
	.72	.51	173	89	.80

TABLE V (continued)

Date	Length $l/l_o$	Relative Tension $(P_o)/P_o$	Stiffness $(P_o)/l_o$	Stiffness $P_o/l_o$	Relative Stiffness $S_l/S_{l_o}$
3. v. 72	1.0	1.0	101	101	1.0
	.92	.91	112	102	1.02
	.84	.73	131	96	.96
	.80	.66	140	92	.92
	.76	.44	172	76	.76
5. v. 72	1.0	1.0	92	92	1.0
	.87	.90	102	92	1.0
	.83	.80	112	90	.98
	.80	.67	127	85	.92
	.77	.54	138	74	.81
	.73	.37	170	63	.68
	.70	.23	196	45	.49
16. v. 72	1.0	1.0	108	108	1.0
	.88	.90	118	106	.97
	.80	.70	132	92	.84
	.76	.55	149	82	.75
	.71	.40	167	66	.60

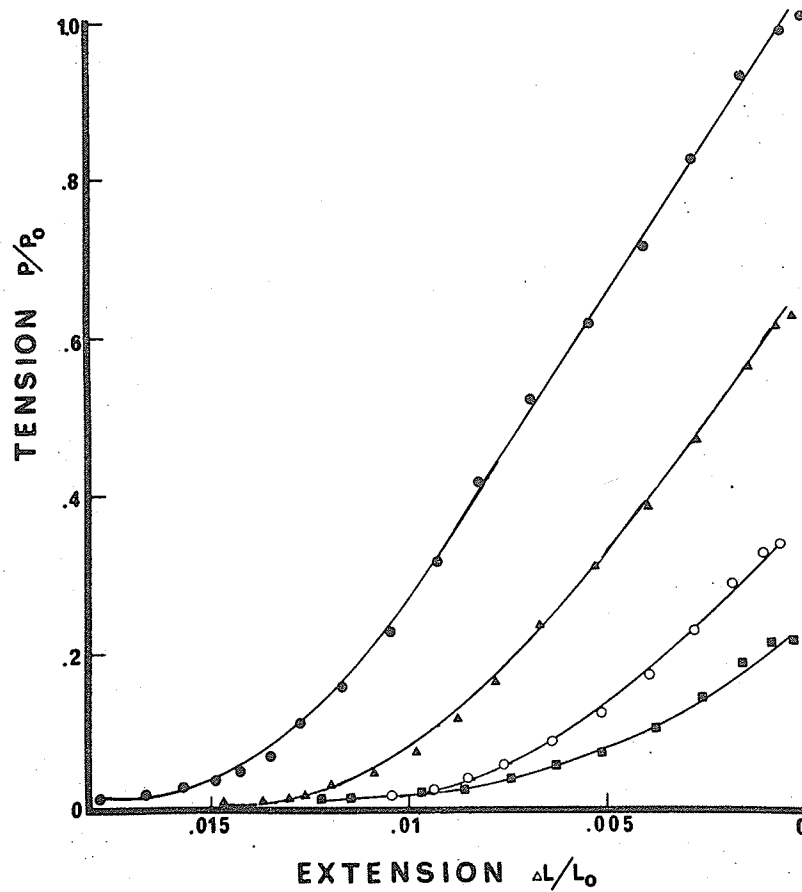


Figure 15: Tension-extension curves from maximum tetanic tension in a toad sartorius at four different lengths,  $\bullet = l_0$ ,  $\blacktriangle = .8 l_0$ ,  $\circ = .72 l_0$ ,  $\blacksquare = .68 l_0$ . The stiffness values for these curves are  $77 P_0/l_0$  ( $l_0$  curve),  $63 P_0/l_0$  ( $.8 l_0$  curve),  $50 P_0/l_0$  ( $.72 l_0$  curve),  $37 P_0/l_0$  ( $.68 l_0$  curve). These curves do not superimpose on the  $l_0$  curve if shifted along the abscissa so that the point  $(P_0)_l$  falls on the curve at body length. For this muscle  $l_0 = 25$  mm, wt. = 67 mg.



stiffness and length is shown in Fig. 16. In Fig. 17 the stiffness points are pooled and are compared with the corresponding points of the tension-length relation for these same muscles. The stiffness of the muscle remains at maximum for a short distance while the tension is falling and then from about  $.8 l_0$  the stiffness and tension curves fall parallel to each other with the stiffness, at a given length, always higher than the force. The relationship between the maximum isometric force at a given length and the stiffness at that length is seen in Fig. 18. To a first approximation, these points are linear to about  $.85 P_0$  where the first sign of a decline in stiffness is observed. It was difficult to obtain stiffness values for points much below  $.7 l_0$  ( $.2 P_0$  in Fig. 18) because of the deterioration of the stimulated muscle, at very short lengths, as it goes into the 'delta' state (Ramsey and Street, 1940). The stiffness-force curve may have an intercept on the stiffness axis or may fall quite sharply to zero at points below about  $.2 P_0$ . The decline in the muscle's stiffness with a corresponding decrease in tension at lengths below  $l_0$  suggests, once again, that the force-generating sites are regions of relatively high compliance.

#### e.) Initial Development of Force

In another series of experiments we have measured the compliance of the contracting muscle during the development of isometric tension at body length ( $l_0$ ). Instead of releasing the muscle from the plateau of a tetanus, quick releases were given at 30, 50, 70, 100 msec etc. after the first shock. The limiting slope of each of the tension-extension plots obtained was then taken

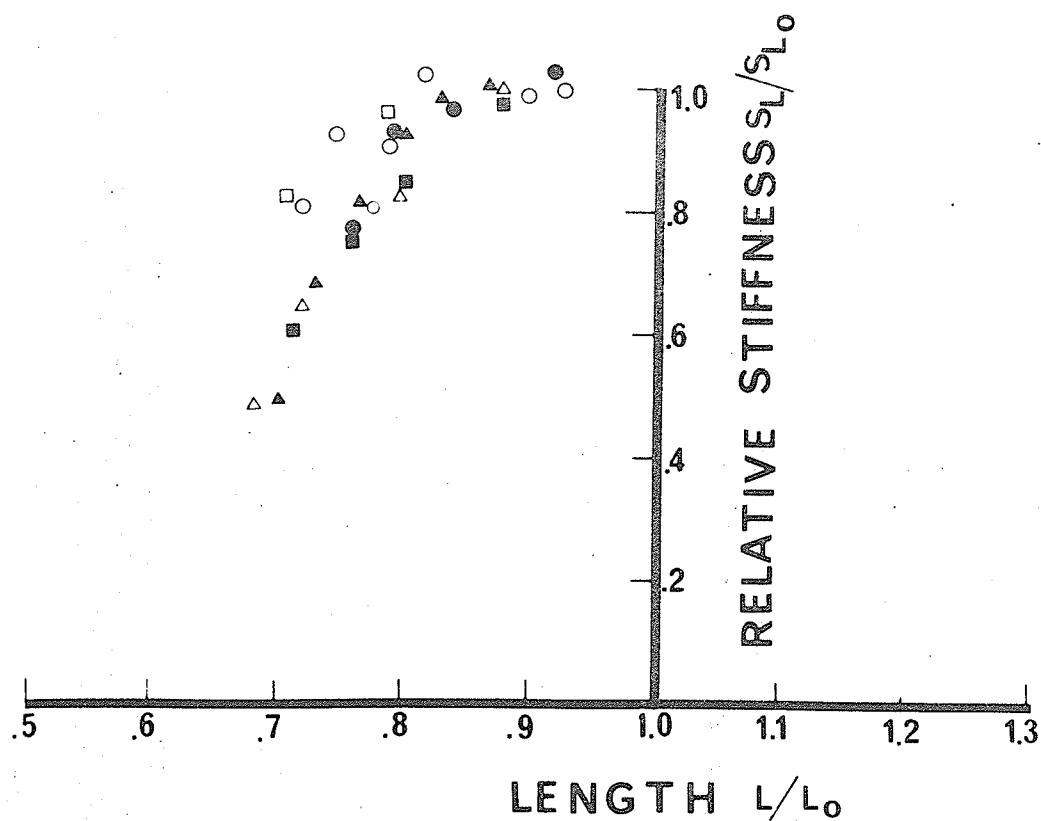


Figure 16: The instantaneous stiffness at maximum isometric tetanic tension in toad sartorii at lengths below  $l_0$ . Different symbols refer to the results of six experiments. Stiffness values normalized with respect to the maximum stiffness at  $l_0$ . Length is expressed as a fraction of  $l_0$ .

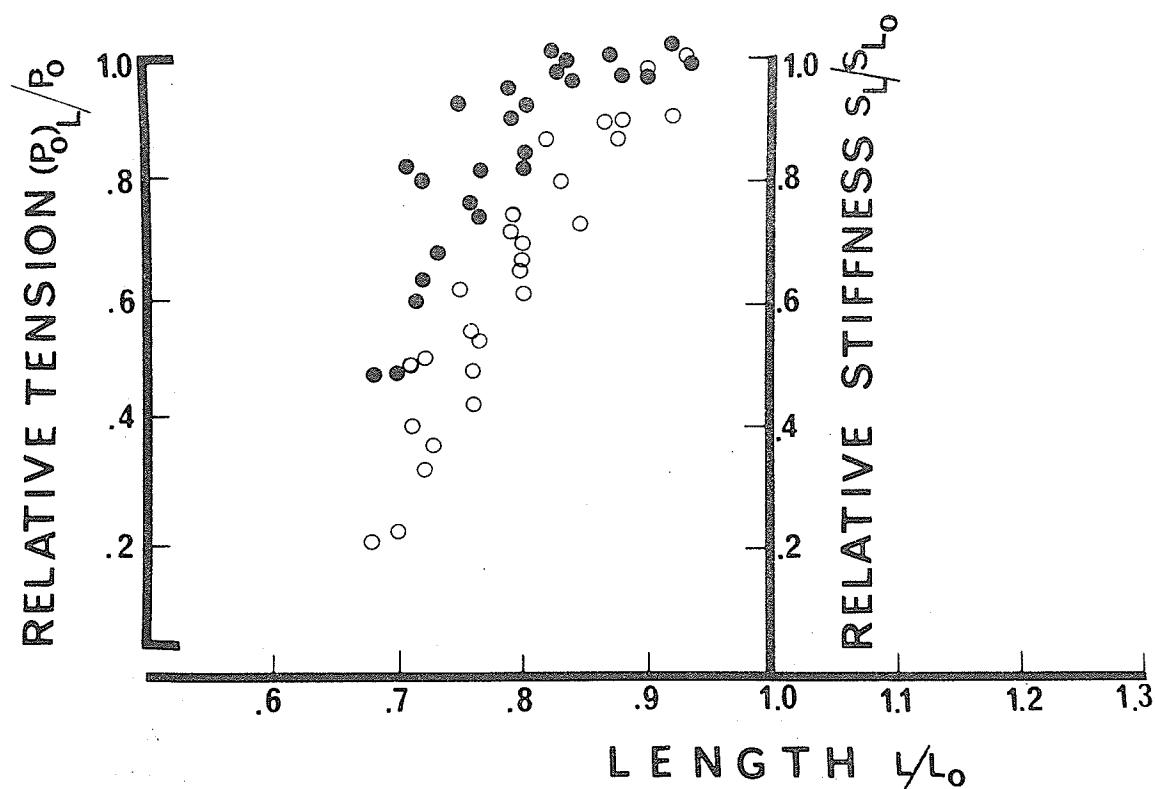


Figure 17: A comparison of the instantaneous stiffness and the maximum tetanic force below body length in toad sartorii. The stiffness values (●) and tension values (○) represent the pooled data from six separate experiments. Stiffness and tension are normalized with respect to their maximum values at body length. Length is expressed as a fraction of  $l_0$ .

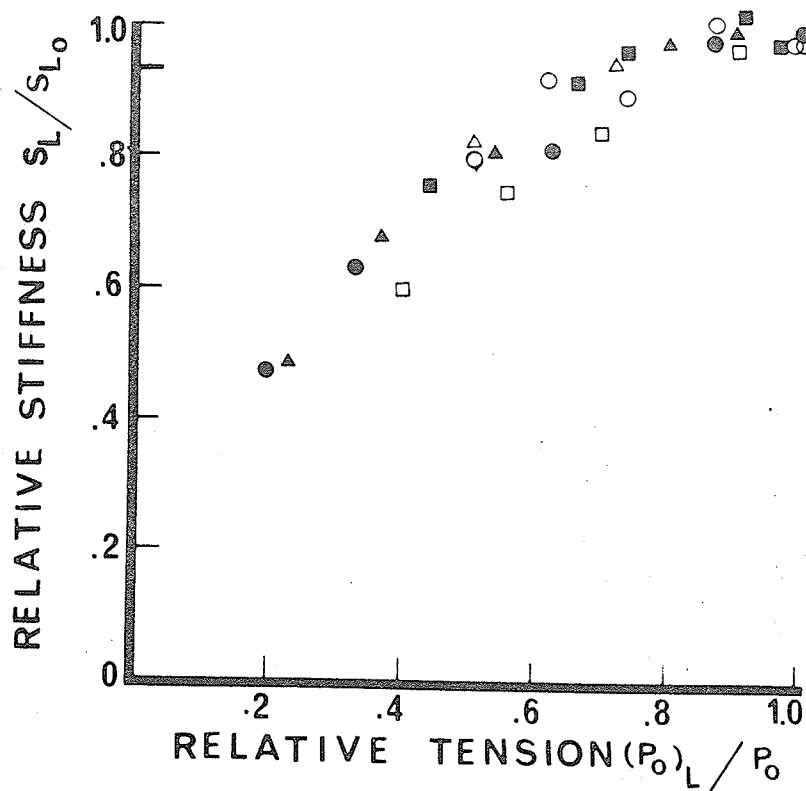


Figure 18: The relation between maximum stiffness and tetanic force in toad sartorii at short lengths. The different symbols refer to results from six separate experiments. Both stiffness and tension are normalized with respect to their maximum values at body length.

as a measure of the stiffness of the muscle corresponding with that time and developed force, i. e. the stiffness which would have existed at that point had there been no release. Each of these releases then yields a single point on a cumulative effective stiffness-force curve. The results of five experiments of this kind are summarized in Table VI and shown in Fig. 19. As before, different symbols represent different experiments. It will be seen that stiffness is again approximately linearly related to developed force giving an exponential tension-extension curve, in contrast with the almost linear "classical" tension-extension curve obtained from a single release from the plateau of a tetanus. This difference is shown in Fig. 20 where Fig. 19 has been integrated graphically to give an "effective" tension-extension curve for direct comparison with eleven directly measured "classical" curves. Clearly the "effective" curve shows a greater compliance, especially in the region of low tension, although the results shown in Fig. 9 suggest a very rapid increase in the stiffness of the stimulated muscle just at the beginning of force development as described by Buchthal and Kaiser (1944) and Hill (1951a). Again this might be expected if active link formation is proceeding at a high rate during the development of force. It may be worth emphasizing here that the "effective" stiffness curve is in no sense to be regarded as the actual tension-extension curve of any real elastic body within the muscle at any time, but is a composite of a succession of such curves, taking a single point from each. It is noteworthy that this behaviour invalidates the use of  $dP/dt$  versus  $P$  plots to measure the state of activation or "active state"

TABLE VI

STIFFNESS AND TENSION VALUES FOR THE TOAD SARTORIUS DURING THE INITIAL DEVELOPMENT OF FORCE

Date	Relative Tension $P/P_o$	Stiffness $P_o/l_o$	Relative Stiffness $S_p/S_{p_o}$
11. ix. 71	.04	18	.28
	.20	29	.45
	.50	46	.71
	.64	54	.83
	.79	52	.80
	.82	62	.95
	1.0	65	1.0
27. ix. 71	.21	26	.37
	.43	37	.53
	.69	55	.79
	.73	56	.80
	.80	55	.79
	1.0	70	1.0
4. x. 71	.19	23	.42
	.41	38	.69
	.56	51	.93

TABLE VI (continued)

Date	Relative Tension $P/P_o$	Stiffness $P_o/l_o$	Relative Stiffness $S_p/S_{p_o}$
13.x.71	.65	50	.91
	.74	50	.91
	.80	51	.93
	.85	54	.98
	1.0	55	1.0
	.06	15	.27
	.22	24	.44
	.41	37	.68
	.50	41	.75
	1.0	55	1.0
13.xii.71	.07	11	.17
	.17	26	.40
	.37	37	.57
	.50	44	.67
	.59	53	.81
	.60	55	.84

TABLE VI (continued)

Date	Relative Tension $P/P_o$	Stiffness $P_o/l_o$	Relative Stiffness $S_p/S_{p_o}$
	.63	50	.76
	.67	56	.86
	.72	55	.84
	1.0	66	1.0



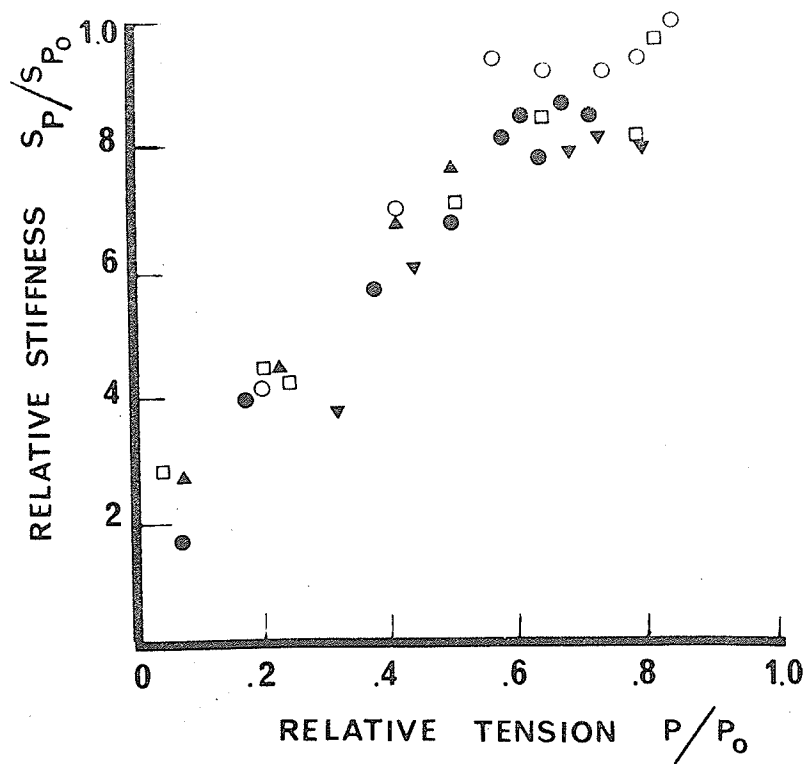


Figure 19: The relation between the relative stiffness during initial force development and the developed tension, in toad sartorii, at  $l_0$ . The different symbols represent results from five separate experiments. The stiffness and force values are expressed as fractions of their values at maximum tetanic tension,  $P_0$ .

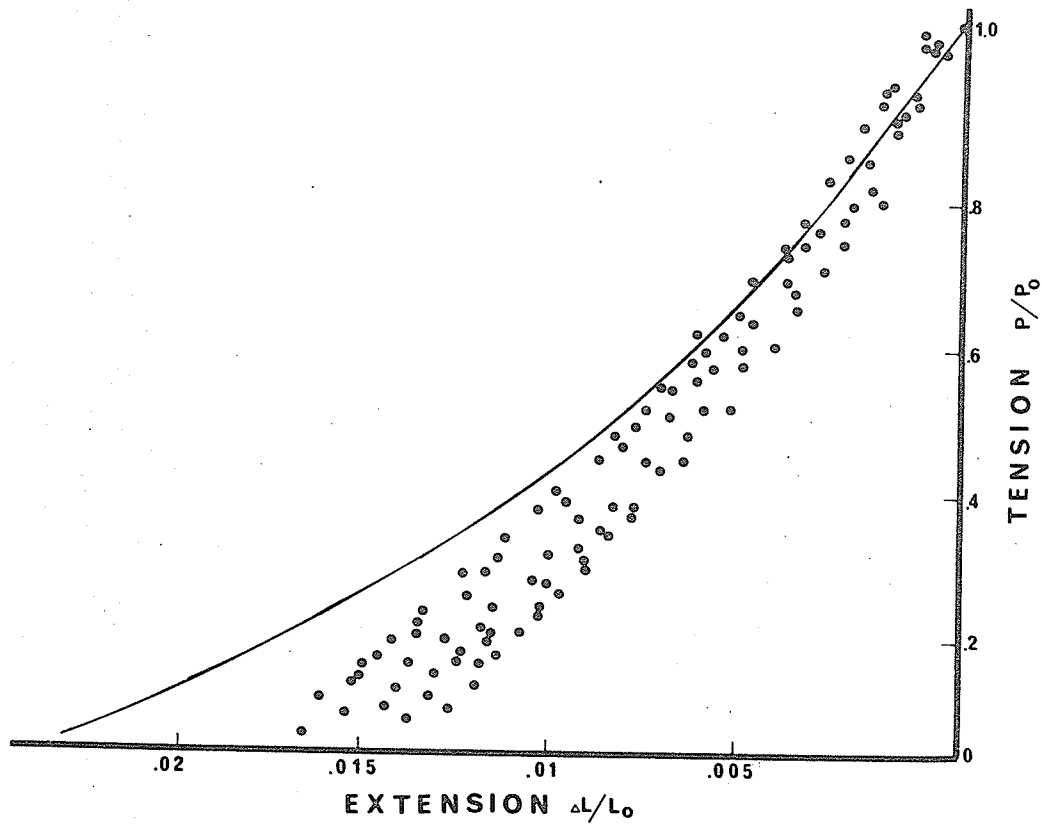


Figure 20: The effective tension-extension curve for toad sartorii at  $l_0$  (continuous line), derived by graphical integration of Fig. 19, compared with eleven classical tension-extension curves obtained by single controlled releases to zero force from peak tetanic tension at  $l_0$ .

intensity (Close, 1963). Such methods assume a constancy on the part of the muscle's elastic properties which does not exist.

### 3. Laser Experiments

The striation spacing for the toad (Bufo bufo) sartorius has never been reported in the literature. Preliminary experiments in our laboratory, using a light diffraction technique, indicates that at  $l_{\max}$  the sarcomere width is  $2.28 \mu$ . This falls within the range of sarcomere widths reported for single fibers of frog semitendinosus (Gordon, Huxley and Julian, 1966b) and for the frog sartorius (Close, 1972). While doing the determinations of sarcomere widths it became apparent that the measured length of the muscles in situ ( $l_0$ ) is always greater than the length at which the maximum tetanic tension is obtained ( $l_{\max}$ ).

Figure 21 shows the distribution of sarcomere widths measured at different muscle lengths. The points have been fitted to a straight line to give a satisfactory agreement between a tension-length curve for the toad sartorius and for the isolated single fiber of the frog semitendinosus. A tension-length curve from two separate toad sartorii preparations (open and closed circles) is shown in Fig. 22. The sarcomere widths measured from our calculated line in Fig. 21 have been placed on the abscissa of Fig. 22. As well, the tension-length curve for a single fiber of the frog semitendinosus (Gordon et al, 1966) has been superimposed (solid line), with a shift of  $0.08\mu$  to the right of  $l_{\max}$ , on our curve. At long lengths there is good agreement between the two muscles whereas at lengths below  $l_{\max}$  there is more rapid decline in tension for the toad muscles.

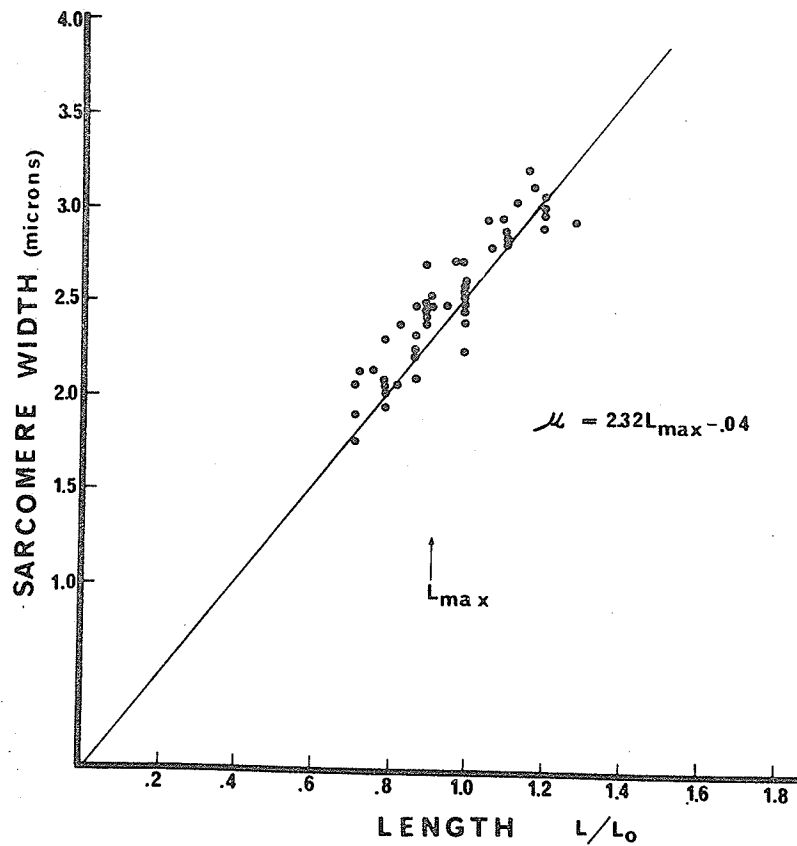


Figure 21: The distribution of measured sarcomere widths from five separate toad sartorii at different lengths. The solid line has been drawn within the limits of the standard deviations of two-way regression lines through the points. The sarcomere width at  $l_{max}$  is  $2.28 \mu$ . The arrow shows the approximate position of  $l_{max}$ .

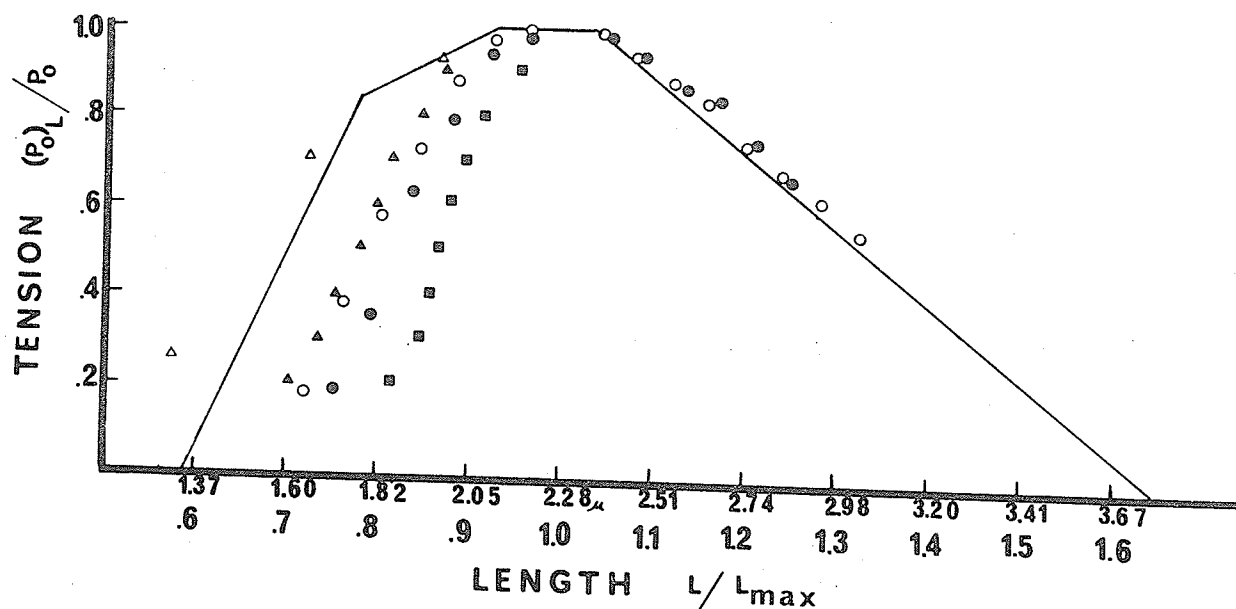


Figure 22: A comparison of tension-length curves. Open and closed circles ( $\circ$ ,  $\bullet$ ) are from two separate toad sartorii. Solid line is tension-length curve for single fiber of frog semitendinosus from Gordon et al (1966). It has been shifted  $0.08\mu$  to the right of  $l_{\max}$ .  $\triangle$  - part of tension-length curve for frog sartorius.  $\blacksquare$  - part of tension length for whole semitendinosus, both from Délèze (1961),  $\triangle$  - part of tension-length curve for frog sartorius from Aubert (1956). Sarcomere widths on abscissa from regression line in Fig. 21.

For further comparison, points from parts of tension-length curves for the frog sartorius muscle (closed triangles) and the frog whole semitendinosus muscle (boxes), published by D  leze (1961), have also been placed on Fig. 22.

The frog sartorius muscle appears to be in good agreement with the toad sartorius, in both cases the tension falling faster than for the single fiber of semitendinosus.

An interesting observation is that in the whole semitendinosus muscle, the tension falls much faster than for a single fiber. The final set of points (open triangles) are again for the frog sartorius from the work of Aubert (1956) in which we see that the tension below  $l_{max}$  decreases at approximately the same rate as for the single fibers. This brings out the fact that the observed discrepancy in tension fall may not be in the validity of the comparison of whole muscle to single fibers. Recently, Close (1972) has pointed out that the twitch:tetanus ratio for whole muscles and single fibers are about the same, which would make the above comparison valid. Moreover he has compared the tension-length curve from Gordon et al for single fibers with the frog sartorius and this time there is excellent agreement at both long and short lengths. It is difficult to interpret the significance of a steeper decline in tension in the whole muscle compared to isolated fibers, if in fact this discrepancy is real. Furthermore, there is obvious variability in the decline in tension between whole muscles at lengths below  $l_0$ . This, in itself, is an interesting and as yet unexplained fact. A similar variation at long lengths does not appear to be evident. Normalizing the tension values with respect to cross-sectional area may help to remove the

discrepancy between whole muscles but would make the situation worse between whole muscles and single fibers. Further insight into the reason for the decline in tension at short lengths may help to resolve this problem (see discussion).

## V. DISCUSSION AND SUMMARY



In Hill's model of muscle contraction the series elastic element does not change its properties during shortening and tension development although more recently, Hill (1970) has calculated that the SEC should stiffen as force development proceeds. The results described here show that the compliance of the active toad sartorius at 0°C depends not only on muscle length, but also alters during the isometric development of force. The greater part of the muscle's compliance appears to be in the sarcomere, in agreement with the recent report of Huxley and Simmons (1971b). These authors have also found a decrease in muscle stiffness at lengths longer than the resting length, corresponding to a decrease in the area of overlap of the myofilaments and thus the number of force-generating cross-links produced on stimulation (Gordon, Huxley and Julian, 1966b). If most of the muscle's compliance were in the tendons then at long lengths the stiffness of the muscle would increase. On the other hand if elements within the sarcomere are the major component of the overall compliance then the observed decrease in stiffness at long lengths would be predicted. Our findings on the changes in the tension-extension curve at short lengths and during the initial development of force in isometric tetani also seem consistent with this idea. Thus it becomes apparent that a muscle's compliance is related to its contractile activity although the nature of this relationship is not yet clear. Huxley and Simmons' (1971b) model of the cross-link possesses both an undamped instantaneous elasticity as well as an element with combined viscous and elastic properties. Despite the relative slowness of our releases (between 3 and 10 msec

from  $P_0$  to zero force) in comparison with those of Huxley and Simmons (1 msec), our tension-extension curves for the toad sartorius most resemble the curve they give for their fast ( $T_1$ ) component. The compliance seen in our experiments must be essentially undamped since the tension-extension curves are not found to be significantly altered by changing the release velocity over a wide range (see Fig. 11).

If the major site of compliance within the muscle is indeed the cross-links, then it follows that the two component model of Hill is no longer tenable in its simple form (although in practice the tendon and compliance of the experimental apparatus will always contribute a true series elastic component which will have the effects described by Hill (1951b)). However it is possible that the major site of compliance within the sarcomere is not the cross-links but the unbonded I-filaments. In this case too the muscle's stiffness would be an increasing function of the area of overlap. Now the two component model could still be applicable, with the modification that the load-extension curve of the series elastic component would have to be taken as varying with the overall muscle length. In principle it is possible to distinguish between these two extreme hypotheses since they predict different stiffness-length and stiffness- $P_0$  curves. If the major site of compliance were the unbonded I-filaments then the muscle stiffness should be inversely related to I-band width with an abrupt fall to zero when the muscle is so stretched that the I-filaments disengage. On the other hand, the alternate hypothesis, that the I-filaments are comparatively

rigid and that the cross-links (acting in parallel) are the major source of the compliance, predicts that at long lengths there would be a linear fall in stiffness with increasing length, coinciding with the decline in maximum tension.

Figure 23 shows the pooled stiffness- $P_0$  data with the predictions made by these two hypotheses indicated by the solid lines (see Appendix). It is clear that the points are distributed about the unity slope line, which is the predicted line if all the compliance were in the cross-bridges. Moreover x-ray diffraction studies of living muscle indicate that the I-filament length does not increase by more than 0.2% (Huxley and Brown, 1967).

Finally, Aubert (1956) has shown that in a muscle stretched beyond  $l_0$  there is a decrease in the non-labile fraction of the maintenance heat rate which is proportional to  $P_0$  at the new length. Moreover, the maintenance heat rate versus tension points lie on the unity slope line which is similar to our stiffness versus force curve (Fig. 14). The correlation between Aubert's findings and ours suggests that the decline in maintenance heat rate and stiffness at long lengths are both due to a reduction in the total number of active cross-links formed as a result of a decrease in the area of overlap of the myofilaments.

The tension-extension properties of active muscle previously shortened to lengths below  $l_0$  are difficult to interpret because the question of why there is a decline in tension at short lengths is still unresolved. H. E. Huxley (1965) suggested that the thin filaments which penetrate into the center of the A band at short lengths would have an abnormal orientation with respect to the adjacent

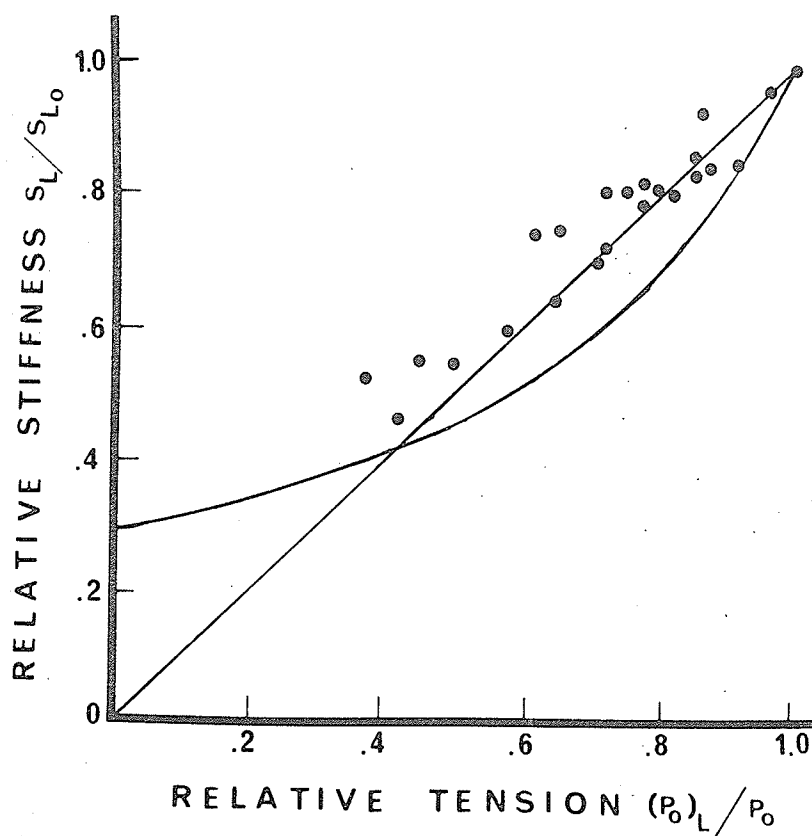


Figure 23: The relation between maximum stiffness and tetanic force in toad sartorii at long lengths (same as Fig. 14). The values from nine separate experiments are pooled. Unity slope line (a) is the predicted relation between force and stiffness if all the compliance were in the cross-bridges. The line (b) shows the predicted relationship if all the compliance were in the I-band. For calculation of lines, lengths of thick and thin filaments were taken as  $1.6\mu$  and  $1.0\mu$  respectively and sarcomere width at  $l_0$  equal to  $2.25\mu$ .

cross-bridges. Such a region would not produce any tension and might interfere mechanically and chemically with correctly oriented actin and myosin filaments. Thus, even though the area of overlap is increasing at short lengths, the new geometrical arrangement of the myosin to actin molecules (12 actins around 1 myosin) retards force development. This is based on the underlying assumption that the force produced by a muscle reflects the total number of active force-generating cross-bridges formed at any one time (Huxley, 1957). In line with this, Takauji and Honig (1972) have shown a decrease in ATPase activity at sarcomere lengths below the optimum, in isolated myofibrils of rat heart. This implies that there is a decrease in the ability of the actomyosin sites to utilize the energy of ATP to perform mechanical work at short lengths. As well, a decline in the duration of the active state in single fibers at short lengths has been observed by Edman and Kiessling (1970). Furthermore a decrease in the non-labile fraction of the maintenance heat rate (which can be considered to represent contractile activity) of isometric tetani at lengths below  $l_0$  has been reported by Aubert (1956). However, at short lengths, Aubert found a relatively large non-labile maintenance heat rate even though the tension was greatly reduced. Similarly we have seen that the stiffness at a given length ( $l < l_0$ ) is always greater than the maximum developed force (refer to Fig. 17). Both of these results can be explained by assuming that there was a force within the muscle that opposes shortening. Ramsey and Street (1940) pointed out that a muscle shortened below  $l_0$  will relax to a slack length of  $2.1 \mu$  suggesting that there was

an internal force in the muscle tending to extend it. Such a force would naturally subtract from the tension produced by the myofilaments. Evidence for such a force has been provided by Gordon, Huxley and Julian (1966b) who have calculated an increase in internal osmotic pressure of  $1 \text{ kg/cm}^2$  in a muscle shortened from 40-75% of its initial length. This corresponds to a force of about  $.3 P_0$  in isolated fibers from frog semitendinosus. Additional evidence has recently been provided by Simmons (1970) who has shown that single fibers allowed to shorten freely in solutions of increasing tonicity exhibit a definite resistance to shortening at sarcomere lengths of  $2.0 \mu$  and  $1.92 - 1.95 \mu$ . The first plateau ( $2.0 \mu$ ) corresponds to an interaction of the ends of the thin filaments (Brown, Gonzalez-Serratos and Huxley, 1970) and the second plateau ( $1.93 \mu$ ) relates to the most recent estimate of the I-filament length (H. E. Huxley and Page as quoted by Simmons). Below  $1.6 \mu$  the decrease in contractility has been attributed to the myosin filaments making contact with the Z-lines. More recently Taylor and Rudel (1970) have proposed that below  $1.6 \mu$  there is an inactivation of the myofibrils close to the center of a muscle fiber. At these short lengths the axial myofibrils become wavy. Rudel and Taylor (1971) have exposed single muscle fibers to subthreshold concentrations of caffeine which potentiates the maximum tetanic tension at short lengths coincident with a disappearance of wavy central myofibrils. It would be interesting to see if similar concentrations of caffeine would potentiate the maximum measured instantaneous stiffness at short lengths.

The preceding evidence leads to the general conclusion that the decline in maximum tetanic force at lengths below  $l_{\max}$  may be correlated with a decrease in the total number of positive force-generating cross-links. Therefore, in terms of the hypothesis that active cross-links are regions of relatively high compliance a decrease in instantaneous stiffness at lengths below  $l_{\max}$  is expected.

From the point of view of the two component model the difference between the "effective SEC curve" and the tension-extension curve of tetanised muscle is in the right direction to resolve the long-standing problem of the synthesis of the myogram from force-velocity and stress-strain data. Preliminary calculations suggest that use of the effective compliance curve rather than the classical one still makes the predicted myogram rise more rapidly than the observed one, but the difference is greatly diminished (Fig. 24).

The force-velocity experiments are interesting in the light of similarity of many muscles between the product  $a \cdot b$  and the maintenance heat rate in a prolonged tetanus (Hill and Woledge, 1962; Woledge, 1968). This identity does not appear to hold for toad muscle at  $0^{\circ}\text{C}$ . The maintenance heat rate of toad *sartorii* is about 0.4 of that in the frog (Hill and Woledge, 1962; Woledge 1971) while comparison of the toad  $a \cdot b$  product from our results ( $.062 P_0 l_0 / \text{sec}$ ) with the values for the frog given by Hill (1938) and Katz (1939), ( $.082 P_0 l_0 / \text{sec}$ ) gives a ratio of almost 0.8:1. Also, the intrinsic speeds ( $V_{\max}$ ) of both muscles appear to be in the same ratio;  $1.27 l_0 / \text{sec}$  for the toad *sartorii* as compared with  $1.31 l_0 / \text{sec}$  for the frog. This is curious in view of the substantially slower

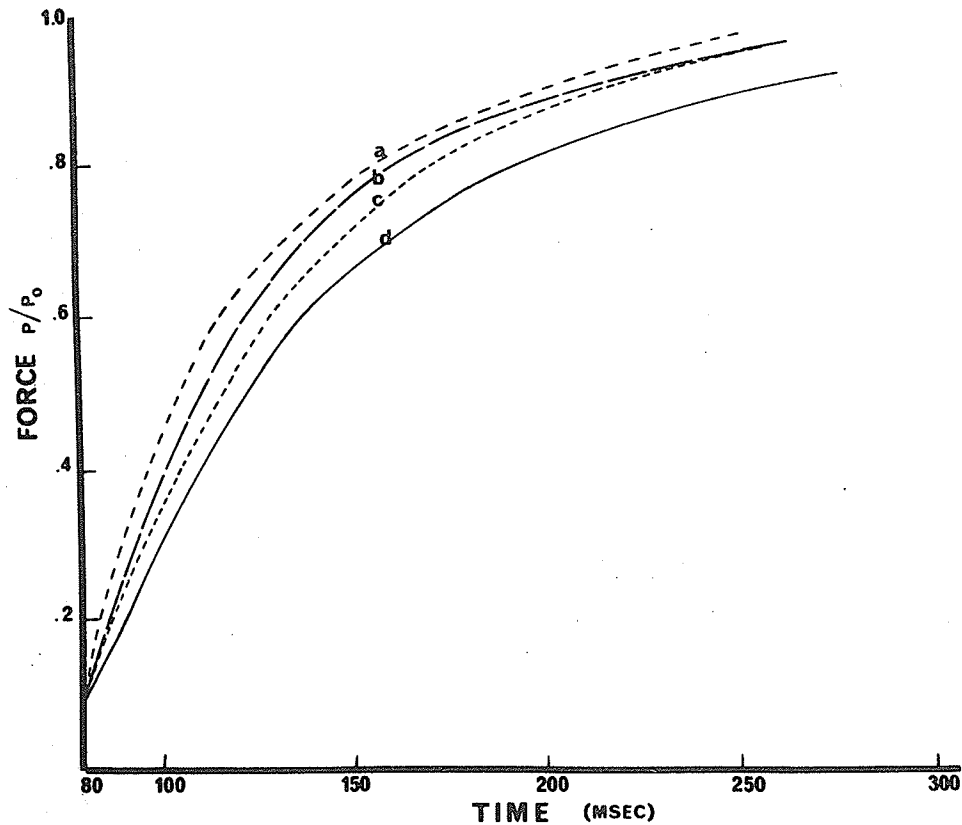


Figure 24: Isometric myograms. Curve d is the observed initial development of isometric tetanic tension in a toad sartorius at 0°C and curve b is the observed redevelopment of isometric tension after release from  $P_0$  to zero force. Curves a and c are the predicted redevelopment and initial development of tension respectively calculated from the force-velocity curve of Fig. 8 and the effective series compliance curve of Fig. 20. Note the calculated initial development of tension curve falls between the observed initial development and redevelopment curves. Calculation begins at  $.1 P_0$ .



development of force in isometric contractions of toad sartorii (Hill, 1970).

Finally, it is hoped that the results presented here will stimulate a revision of traditional active state theory, which relies heavily on the constancy of the SEC during an isometric twitch or tetanus. If indeed, the "series elastic component" is a characteristic of the contractile element itself, then the rise time of the active state will be heavily influenced by the changes in muscle stiffness during the initial development of force (Fig. 19).

## SUMMARY

1. The method of controlled releases was used to obtain tension-extension curves in toad (Bufo bufo) sartorii under a variety of conditions at 0°.
2. The curves obtained were approximately linear over a considerable range of force ( $0.4 P_O$  to  $P_O$ ) if the releases were given from the plateau of tetanic tension. The slope of this linear region was little affected by changes of release velocity in the range 10 to 120 mm/sec.
3. Such changes as did occur with alterations in release velocity could be quantitatively accounted for in terms of the internal shortening predicted by A.V. Hill's two component model.
4. As the muscles were stretched above  $l_O$ , it was found that the maximum stiffness of the tetanised muscles fell in much the same way as the maximum developed force,  $P_O$ .
5. In muscles at lengths below  $l_O$ , there was a similar decrease in the maximum stiffness of the tetanised muscle, though the measured stiffness was always slightly higher than the maximum developed force,  $(P_O)_l/P_O$ .
6. In another series of experiments a rapid change in the overall shape of the tension-extension curve during the early phase of force development in an isometric tetanus was observed. The stiffness of the muscle increased with increasing developed force during this period.
7. The force velocity curve in these muscles was measured by two methods, both giving a similar result. Surprisingly, toad muscle appears to have

about the same intrinsic speed as frog muscle at  $0^\circ$  ( $a/P_0 = .22$ ;  $b/l_0 = .28$ ). The  $a \cdot b$  product from these experiments is considerably greater than the reported values for the maintenance heat rate at  $0^\circ$  in these muscles.

8. The sarcomere width for the toad sartorius, measured with a light diffraction technique was  $2.28 \mu$  at  $l_{\max}$ .
9. The probable site of the variable compliance in active muscle is discussed. It seems most likely that this is within the A-band, perhaps in the cross-bridges themselves.

## VI. BIBLIOGRAPHY

- ABBOTT, B. C. & LOWY, I. (1958). Contraction in molluscan smooth muscle. *J. Physiol.* 141: 385-397.
- ABBOTT, B. C. & MOMMAERTS, W. F. H. M. (1959). Study of inotropic mechanisms in the papillary muscle preparation. *J. gen. Physiol.* 42: 533-551.
- ABBOTT, B. C. & WILKIE, D. R. (1953). The relation between velocity of shortening and the tension-length curve of skeletal muscle. *J. Physiol.* 120: 214-223.
- ADRIAN, R. H. (1956). The effect of internal and external potassium concentration on the membrane potential of frog muscle. *J. Physiol.* 133: 631-658.
- ARMSTRONG, C. F., HUXLEY, A. F. & JULIAN, F. J. (1966). Oscillatory responses in frog skeletal muscle fibres. *J. Physiol.* 186: 26P.
- AUBERT, X. (1956). *Le couplage energetique de la contraction musculaire.* Editions Arscia, Bruxelles.
- BANUS, M. G. & ZETLIN, A. M. (1938). The relation of isometric tension to length in skeletal muscle. *J. cell. comp. Physiol.* 12: 403-420.
- BLANGÉ, T., KAREMAKER, J. M., & KRAMER, A. E. J. L. (1972). Tension transients after quick release in rat and frog skeletal muscle. *Nature* 237: 281-283.
- BOUCKAERT, J. P., CAPELLEN, L. & DE BLENDE, J. (1930). The visco-elastic properties of frog's muscles. *J. Physiol.* 69: 473-492.

- BROWN, L. M. , GONZALEZ-SERRATOS, H. , & HUXLEY, A. F. (1970).  
Electron microscopy of frog muscle fibres in extreme passive shortening.  
J. Physiol. 208: 86-88P.
- BUCHTHAL, F. & KAISER, E. (1944). Factors determining tension development  
in skeletal muscle. Acta. physiol. scand. 8: 38-74.
- BUCHTHAL, F. , KAISER, E. & KNAPPEIS, G. G. (1944). Elasticity, viscosity  
and plasticity in the cross striated muscle fibre. Acta. physiol. scand.  
8, 16-37.
- CAPLAN, S. R. (1966). A characteristic of self-regulated linear energy con-  
verters. The Hill force-velocity relation for muscle. J. theoret. Biol.  
11: 63-86.
- CASELLA, C. (1950). Tensile force in striated muscle, isolated fibre and  
sarcolemma. Acta. physiol. scand. 21: 380-401.
- CIVAN, M. M. & PODOLSKY, R. J. (1966). Contraction kinetics of striated  
muscle fibres following quick changes in load. J. Physiol. 184: 511-534.
- CLINCH, N. F. & BRESSLER, B. H. (1971). The series compliance of toad  
skeletal muscle. Physiologie Canada, 2: 11.
- CLINCH, N. F. & TENNANT, V. A. (1972). A loudspeaker servo system for  
use in studying muscle mechanics. J. appl. Physiol. 32: 703-705.
- CLOSE, R. I. (1972). The relations between sarcomere length and characteristics  
of isometric twitch contractions of frog sartorius muscle. J. Physiol.  
220: 745-762.

- CLOSE, R. (1963). The pattern of activation in the sartorius muscle of the frog. *J. gen. Physiol.* 46: 1-18.
- DÉLEZE, J. B. (1961). The mechanical properties of the semitendinosus muscle at lengths greater than its length in the body. *J. Physiol.* 158: 154-164.
- EDMAN, K. A. P. & KIESSLING, A. (1970). The time course of the active state in relation to sarcomere length and movement studied in single muscle fibres of the frog. *Acta. physiol. scand.* 81: 182-196.
- ELLIOTT, G. F., LOWY, J., & MILLMAN, B. M. (1965). X-ray diffraction from living striated muscle during contraction. *Nature*, 206: 1357-58.
- FENN, W. O. (1923). Quantitative comparison between the energy liberated and the work performed by the isolated sartorius muscle of the frog. *J. Physiol.* 58: 175-203.
- FENN, W. O. (1924). Relation between work performed and energy liberated in muscular contraction. *J. Physiol.* 58: 373-395.
- FENN, W. O. & MARSH, B. S. (1935). Muscular force at different speeds of shortening. *J. Physiol.* 85: 277-297.
- GASSER, H. S. AND HILL, A. V. (1924). Dynamics of muscular contraction. *Proc. Roy. Soc. B*, 96: 398-437.
- GORDON, A. M., HUXLEY, A. F. & JULIAN, F. J. (1966a). Tension development in highly stretched vertebrate muscle fibres. *J. Physiol.* 184: 143-169.

- GORDAN, A. M. , HUXLEY, A. F. & JULIAN, F. J. (1966b). The variation in isometric tension with sarcomere length in vertebrate muscle fibres. *J. Physiol.* 184: 170-193.
- HILL, A. V. (1922). The maximum work and mechanical efficiency of human muscles and their most economical speed. *J. Physiol.* 56: 19-41.
- HILL, A. V. (1938). The heat of shortening and the dynamic constants of muscle. *Proc. Roy. Soc. B*, 126: 136-195.
- HILL, A. V. (1939). The transformation of energy and the mechanical work of muscles. *Proc. Phys. Soc.* 51: 1-18.
- HILL, A. V. (1949). The abrupt transition from rest to activity in muscle. *Proc. Roy. Soc. B*, 136: 399-420.
- HILL, A. V. (1950a). Mechanics of the contractile element of muscle. *Nature* 166: 415-419.
- HILL, A. V. (1950b). The series elastic component of muscle. *Proc. Roy. Soc. B*, 137: 273-280.
- HILL, A. V. (1951a). The effect of series compliance on the tension developed in a muscle twitch. *Proc. Roy. Soc. B*, 138: 325-329.
- HILL, A. V. (1951b). The earliest manifestation of the mechanical response of striated muscle. *Proc. Roy. Soc. B*, 138: 339-348.
- HILL, A. V. (1953a). The 'plateau' of full activity during a muscle twitch. *Proc. Roy. Soc. B*, 141: 498-503.



- HILL, A. V. (1953b). The mechanics of active muscle. *Proc. Roy. Soc. B*, 141: 104-117.
- HILL, A. V. (1965). *Trails and Trials in Physiology*. Edward Arnold Ltd., London.
- HILL, A. V. (1970). *First and Last Experiments in Muscle Mechanics*. Cambridge: Cambridge University Press.
- HILL, A. V. & HARTREE, W. (1920). The thermo-elastic properties of muscle. *Roy. Soc. Lond. Phil. Trans. B*, 210: 153-173.
- HILL, A. V., LONG, C. N. H. & LUPTON, H. (1924). The effect of fatigue on the relation between the work and speed, in the contraction of human arm muscles. *J. Physiol.* 58: 334-337.
- HILL, A. V. & WOLODGE, R. C. (1962). An examination of absolute values in myothermic measurements. *J. Physiol.* 162: 311-333.
- HILL, D. K. (1968). Tension due to interaction between the sliding filaments in resting striated muscle. The effect of stimulation. *J. Physiol.* 199: 637-684.
- HOMSHER, E. & BRIGGS, F. N. (1968). Effects of hypertonicity on calcium fluxes in frog sartorius muscles. *Fed. Proc.* 27: 375.
- HUXLEY, A. F. (1957). Muscle structure and theories of contraction. *Prog. Biophys. biophys. Chem.* 7:255-318.
- HUXLEY, A. F. & NEIDERGERKE, R. (1954). Structural changes in muscle during contraction: Interference microscopy of living muscle fibres. *Nature* 173: 971-973.

- HUXLEY, A. F. & SIMMONS, R. M. (1970). A quick phase in the series elastic component of striated muscle, demonstrated in isolated muscle fibres from the frog. *J. Physiol.* 208: 52P.
- HUXLEY, A. F. & SIMMONS, R. M. (1971a). Mechanical properties of the cross-bridges of frog striated muscle. *J. Physiol.* 218: 59P.
- HUXLEY, A. F. & SIMMONS, R. M. (1971b). Proposed mechanism of force generation in striated muscle. *Nature* 233: 533-538.
- HUXLEY, H. E. (1965). The mechanism of muscular contraction. *Sci. Am.* 213: 18-27.
- HUXLEY, H. E. & BROWN, W. (1967). The low-angle x-ray diagram of vertebrate striated muscle and its behavior during contraction and rigor. *J. molec. Biol.* 30: 383-434.
- HUXLEY, H. E., BROWN W., & HOLMES, K. C. (1965). Constancy of axial spacings in frog sartorius muscle during contraction. *Nature* 206: 1358.
- HUXLEY, H. E. & HANSON, J. (1954). Changes in the cross-striations of muscle during contraction and stretch and their structural interpretation. *Nature* 173: 973-977.
- JEWELL, B. R. & WILKIE, D. R. (1958). An analysis of the mechanical components in frog's striated muscle. *J. Physiol.* 143: 515-540.
- JULIAN, F. J. (1971). The effect of calcium on the force-velocity relation of briefly glycerinated frog muscle fibres. *J. Physiol.* 218: 117-147.

KATZ, B. (1939). The relation between force and speed in muscular contraction.  
J. Physiol. 96: 45-64.

LEVIN, A. & WYMAN, J. (1927). The viscous elastic properties of muscle.  
Proc. Roy. Soc. B, 101: 218-243.

LUPTON, H. (1923). The relation between the external work produced and the  
time occupied in a single muscular contraction in man. J. Physiol.  
57: 68-75.

MATSUMOTO, Y. (1967). Validity of the force-velocity relation for muscle  
contraction in the length region,  $l \leq l_0$ . J. gen. Physiol. 50: 1125-  
1137.

NATORI, R. (1954). The property and contraction process of isolated myofibrils.  
Jikeikai med. J. 1: 119-126.

PAGE, S. G. & HUXLEY, H. E. (1963). Filament lengths in striated muscle.  
J. cell. Biol. 19: 369-390.

PARMELY, W. W. & SONNENBLICK, E. H. (1967). Series elasticity in heart  
muscle. It's relation to contractile element velocity and proposed muscle  
models. Circulation Res. 20: 112-123.

PARMLEY, W. W., YEATMAN, L. A. & SONNENBLICK, E. H. (1970).  
Differences between isotonic and isometric force-velocity relations in  
cardiac and skeletal muscle. Am. J. Physiol. 219: 546-550.

PODOLSKY, R. J. (1959). The chemical thermodynamics and molecular mechan-  
isms of muscular contraction. Ann. N.Y. Acad. Sci. 72: 522-537.

- PODOLSKY, R. J. (1961). In: Biophysics of Physiological and Pharmacological Actions, A. M. Shanes, editor. Washington, D.C.
- PODOLSKY, R. J. (1964). The maximum sarcomere length for contraction of isolated myofibrils. *J. Physiol.* 170: 110-123.
- RAMSEY, R. W. & STREET, S. F. (1940). The isometric length-tension diagram of isolated muscle fibres of the frog. *J. cell. comp. Physiol.* 15: 11-34.
- RAPOPORT, S. I. (1972). Mechanical properties of the sarcolemma and myoplasm in frog muscle as a function of sarcomere length. *J. gen. Physiol.* 59: 559-585.
- RITCHIE, J. M. (1954). The effect of nitrate on the active state of muscle. *J. Physiol.* 126: 155-169.
- RITCHIE, J. M. , WILKIE, D. R. (1958). The dynamics of muscular contraction. *J. Physiol.* 143: 104-113.
- RUDEL, R. , TAYLOR, S. R. (1971). Striated muscle fibers: facilitation of contraction at short lengths by caffeine. *Science* 172: 387-388.
- SANDOW, A. (1961). In: Biophysics of Physiological and Pharmacological Actions. Abraham M. Shanes, editor. Energetics of Muscular Contraction, pg. 413. Published by American Association for the Advancement of Science, Washington, D.C.
- SHADLER, M. , STEIGER, G. J. & RUEGG, J. C. (1971). Mechanical activation and isometric oscillation in insect fibrillar muscle. *Pflügers Arch.* 330: 217-229.

- SIMMONS, R. M. (1970). Resistance to shortening at I-filament lengths in frog muscle fibres. *J. Physiol.* 212: 20P.
- SONNENBLICK, E. H. (1962). Implications of muscle mechanics in the heart. *Fed. Proc.* 21: 975-990.
- SONNENBLICK, E. H. (1964). Series elastic and contractile elements in heart muscle: changes in muscle length. *Am. J. Physiol.* 207: 1330-1338.
- STEPHENS, N. L. & KROMER, U. (1971). Series elastic component of tracheal smooth muscle. *Am. J. Physiol.* 220: 1890-1895.
- TAKAUJI, M. & HONIG, C. R. (1972). Shortening and ATPase activities of single cardiac fibrils of normal sarcomere length. *Am. J. Physiol.* 222: 1-9.
- TAYLOR, S. R. , RUDEL, R. (1970). Striated muscle fibres: inactivation of contraction induced by shortening. *Science* 167: 882-884.
- WILKIE, D. R. (1950). The relation between force and velocity in human muscle. *J. Physiol.* 110: 249-280.
- WILKIE, D. R. (1956). Measurement of the series elastic component at various times during a single muscle twitch. *J. Physiol.* 134: 527-530.
- WOLEDGE, R. C. (1968). The thermoelastic effect of change of tension in active muscle. *J. Physiol.* 155: 187-208.
- WOLEDGE, R. C. (1971). Heat production and chemical change in muscle. *Prog. Biophys. molec. Biol.* 22: 39-74.

## VII. APPENDIX

1. Calculation of a stiffness-force curve based on the prediction that all of an active muscle's instantaneous elasticity is in the unbonded I-filament.

Stiffness  $\propto$  1/I-band width

I-band width = 1/2 sarcomere width - 1/2 A-band width.

For purposes of computation the following values are taken:

Thick filament length =  $1.6 \mu$

Thin filament length in a half sarcomere =  $1.0 \mu$

Sarcomere width at  $l_0 = 2.25 \mu$ .

The stiffness values are determined by calculating the reciprocal of the I-band width at various sarcomere lengths (Table VII). The stiffness values are normalized with respect to the stiffness at  $P_0$  for comparison with the experimental stiffness-force curve.

TABLE VII  
CALCULATED STIFFNESS AT DIFFERENT SARCOMERE LENGTHS  
IF ALL THE STIFFNESS WERE IN THE I-BAND

*Force ( $P_o$ )/ $P_o$	**Sarcomere Length (microns)	1/2 Sarcomere Length (microns)	I-Band Width (microns)	*Normalized Stiffness $S_p/S_{p_o}$
$P_o$	2.25	1.125	0.325	1.0
0	3.65	1.825	1.025	.317
.1	3.47	1.735	.935	.348
.2	3.34	1.672	.872	.373
.3	3.23	1.619	.819	.397
.4	3.097	1.549	.749	.434
.5	3.00	1.500	.700	.464
.6	2.838	1.419	.619	.525
.7	2.676	1.338	.538	.604
.8	2.573	1.287	.487	.667
.9	2.397	1.985	.399	.815

\*The relation between the force and the stiffness at long lengths shown as the curved line in Fig. 23.

\*\*Measured from the tension-length curve for single fibers of the frog semitendinosus in Gordon et al (1966b, pg. 185).



2. Calculation of a stiffness-force curve based on the prediction that all of the instantaneous elasticity of an active muscle is in the area of overlap of the thick and thin filaments, i.e. in the cross-bridges.

The same values for the filament lengths and sarcomere width at  $l_o$  as in Appendix I are used.

Stiffness  $\propto$  area of overlap (OA)

OA = I-filament length - I-band width.

Stiffness at  $(P_o)_l = P_o$  is taken as 1.

Data is summarized in Table VIII.

TABLE VIII  
CALCULATED STIFFNESS AT DIFFERENT SARCOMERE LENGTHS  
IF ALL THE STIFFNESS WERE IN THE CROSS-BRIDGES

*Force ( $P_o$ )/ $P_o$	**Sarcomere Length (microns)	I-Band Width (microns)	Area of Overlap (microns)	*Normalized Stiffness $S_p/S_{p_o}$
$P_o$	2.25	0.325	.675	1.0
0	3.65	1.025	0	0
.1	3.47	.935	.065	.096
.2	3.34	.872	.128	.190
.3	3.23	.819	.181	.268
.4	3.097	.749	.251	.372
.5	3.00	.700	.300	.444
.6	2.838	.619	.381	.564
.7	.2676	.538	.462	.684
.8	2.573	.487	.513	.760
.9	2.397	.399	.601	.890

\*The relation between the force and the stiffness at long lengths is shown as the unity slope line in Fig. 23.

\*\*Measured from the tension-length curve for single fibers of frog semitendinosus in Gordon et al (1966b, pg. 185).

# Proposed Mechanism of Force Generation in Striated Muscle

A. F. HUXLEY & R. M. SIMMONS

Department of Physiology, University College London, Gower Street, London WC1

**Recordings of the change in tension in striated muscle after a sudden alteration of the length have made it possible to suggest how the force between the thick and thin muscle filaments may be generated.**

ONE approach to the elucidation of the kinetics of movement of the "cross-bridges" which are widely assumed to generate the relative force between the thick and thin filaments during contraction of a striated muscle fibre is to record and analyse the transient response of stimulated muscle to a sudden change either of tension or of length. Considerable progress has been made in this way by Podolsky and his colleagues<sup>1-3</sup> who recorded the time course of shortening after a sudden reduction in load. Similar responses have been recorded repeatedly in this laboratory but have not been published because we did not succeed in making the tension change sharply enough to distinguish the component of length change that is truly synchronous with the tension change from that which lags behind the tension change. We therefore turned<sup>4</sup> to the inverse type of experiment, in which the length of the fibre is suddenly altered (by  $\pm 0.1$ – $1.5\%$ ) and the time course of the resulting tension change is recorded. The results have led to some fairly definite suggestions about the way in which the cross-bridges may actually produce the force between the thick and thin filaments.

All the experiments were carried out on isolated fibres from the semitendinosus muscle of the frog *Rana temporaria*, at  $0^{\circ}$ – $4^{\circ}$  C. Length changes, complete in less than 1 ms, were produced by means of a servo system<sup>5</sup>, and tension was recorded with a capacitance gauge<sup>6</sup>. Compliance in the apparatus itself is small enough to be completely disregarded; precautions were taken to reduce the compliance in the tendon attachments to a minimum, and in some of the experiments it was eliminated altogether by using the "spot-follower" device<sup>5</sup>, which continuously measures the length of a middle segment of the fibre.

## Responses to Stepwise Length Change

The general time course of tension in these experiments is shown in Fig. 1. This article is concerned only with the changes that occur simultaneously with the length change itself and during the first few milliseconds after it. As has already been briefly reported<sup>4</sup>, these changes are of the kind shown in Fig. 2: the tension undergoes a relatively large alteration simultaneously with the step change of length, but recovers quickly towards a level closer to that which existed before the step. The final recovery to the original tension

place on an altogether slower time scale. The early changes seen in Fig. 2 have only come to light through the improved time resolution of present-day apparatus.

The behaviour shown in Fig. 2 suggests the presence of two structural elements in series. One of these would be an elastic element whose length is altered simultaneously with the change of length that is applied to the whole fibre, thus producing the large initial change of tension. The other would be an element with viscous as well as elastic properties, whose length readjusts itself during the period of a few milliseconds immediately after the length change, as a result of the change in tension. As this readjustment proceeds, the imposed length change comes to be shared between the two structures, giving a tension intermediate between the values immediately before and immediately after the length change. At the time of our first note<sup>4</sup> about this quick initial tension recovery, we thought it likely that the recovery took place by sliding, with movement of the cross-bridges, but that the instantaneous elasticity was mostly in the filaments themselves. Since then we have measured these responses in fibres stretched so as to reduce the amount of overlap between thick and thin filaments. We found<sup>10</sup> that the responses to a given absolute length change were altered only by a reduction in the scale of the tension changes, which varied in direct proportion to the amount of overlap and therefore also to the number of cross-bridges capable of contributing to tension. On these grounds we now believe that the instantaneous elasticity (or at least the greater part of it) resides in the cross-bridges themselves, as well as the structure responsible for the tension recovery.

The relations between length change and tension are illustrated in Fig. 3. The curve  $T_1$  shows the extreme tension reached during the step change of length. It is somewhat non-linear, becoming stiffer with increasing tension as is commonly found in biological materials. This curve is the best experimental approach that we have to the instantaneous elasticity of the fibre, but it is clear from records such as viii-x in Fig. 2 that the tension drop in the larger shortening steps is cut down because the quick recovery has progressed

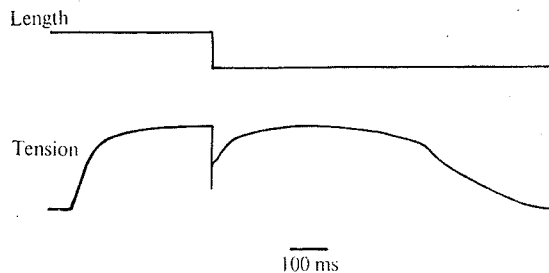
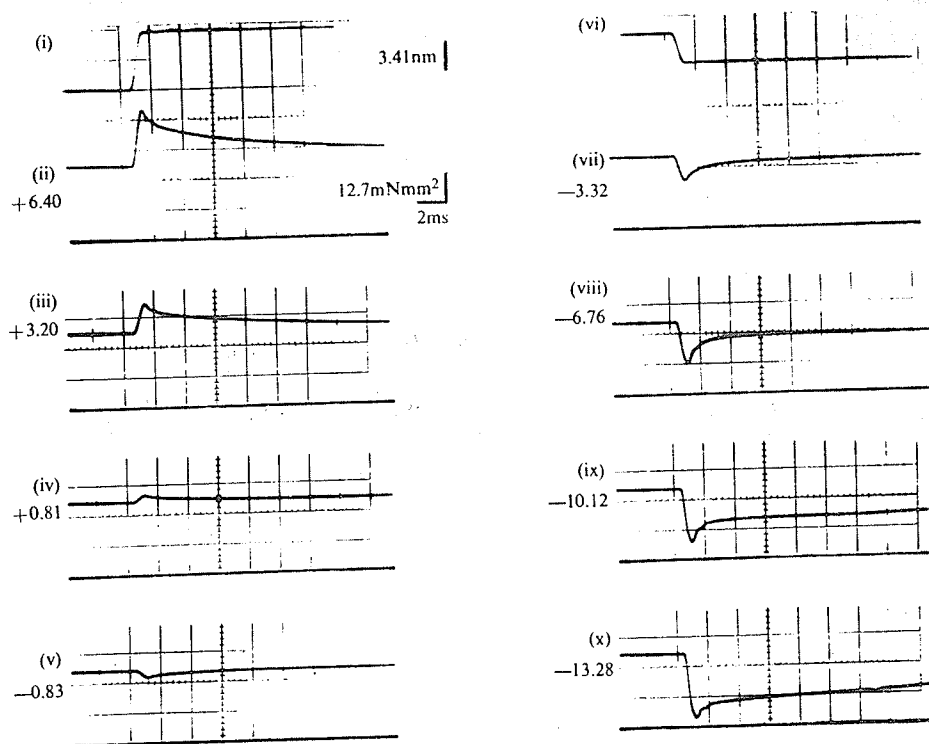


Fig. 1 Isometric tetanus of an isolated muscle fibre (frog,  $4^{\circ}$  C), with an imposed shortening step. This article is concerned with the tension changes during, and in the first few milliseconds after, the length step; these are shown in a full

**Fig. 2** Transient changes in tension exerted by stimulated muscle fibre when suddenly stretched (ii-iv) or shortened (v, vii-x); same experiment as Fig. 1, which shows the whole of the contraction during which record ix was taken. (i) and (vi): records of length change during tension records (ii) and (vii) respectively. The number by each tension record shows the amount of the length change per half-sarcomere, in nm.



to an appreciable extent before the length change is complete. The true curve of the instantaneous elasticity is therefore less curved on the shortening side than the curve of  $T_1$  in Fig. 3; it is even possible that it is practically straight, as indicated by the broken line.

In contrast to this straightforward behaviour of the instantaneous elasticity, the quick tension recovery is highly non-linear both in its extent and in its speed. The line  $T_2$  in Fig. 3 shows the level approached at the end of the quick phase of recovery; for moderate amounts of shortening it has the unusual feature of being concave downwards, reflecting the fact that after a small length step the tension returns practically to its previous level (Fig. 2, iv, v). As regards the time course, it is evident from Fig. 2 that the early tension recovery is much more rapid in releases than in stretches, and that its speed varies continuously over a wide range with the size of the length step. The recovery is not exponential, but an estimate of the dominant rate constant can be obtained and is plotted against the size of the stretch or release in Fig. 4; it is roughly fitted by a curve of the form

$$r = \frac{r_0}{2} (1 + \exp - \alpha y) \quad (1)$$

All these features can be given at least a qualitative explanation if we assume that the force on a cross-bridge influences the length changes in that cross-bridge in the way that is assumed by Eyring and others<sup>11,12</sup> in their theory of the visco-elastic behaviour of high molecular weight polymers. The treatment presented in the following paragraphs is meant only to indicate the way in which these features would emerge from such a theory; a more complete treatment will be needed in order to test whether it is fully consistent with the data.

## Assumptions

The key assumptions that have to be made are (1) that the movement by which a cross-bridge performs work during the period while it is attached takes place in a small number of steps, from one to the next of a series of stable positions with progressively lower potential energy, and (2) that there is a virtually instantaneous elasticity within each cross-bridge

allowing it to shift from one of these stable positions to the next without a simultaneous displacement of the whole thick and thin filaments relative to one another.

These assumptions could be incorporated into some of the mechanisms that have been proposed for the action of the cross-bridges, for example, that of Davies<sup>13</sup>, in which each cross-bridge shortens by folding at a number of points, or that of H. E. Huxley<sup>14</sup>, in which the head of the myosin molecule ( $H$ , Fig. 5) rotates relative to the thin filament, acting as a lever which pulls the thick filament along by a link  $AB$  which is also part of the myosin molecule. Our assumptions fit very conveniently on to H. E. Huxley's proposals, and we shall discuss them on this basis in the way illustrated in Fig. 5. The features shown there which are additional to H. E.

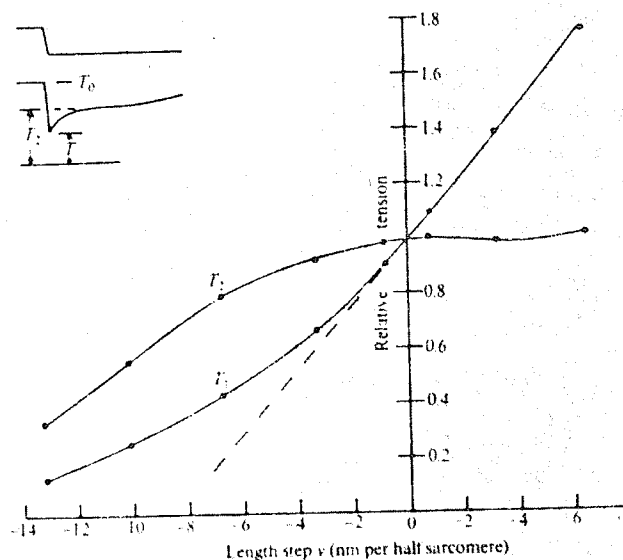


**Fig. 3**  $T_1$ , Extreme tension reached during step, and  $T_2$ , tension approached during quick recovery phase, plotted against amount of sudden stretch (positive) or release (negative). Broken line: extrapolation of the part of the  $T_1$  curve which refers to stretches and small releases. From records in Fig. 2.

Huxley's scheme are as follows. (1) The link  $AB$  is not inextensible as in H. E. Huxley's proposal but contains the instantaneous elasticity which shows up as curve  $T_1$  (Fig. 3). (2) The head has a small number  $s$  of combining sites ( $M_1, M_2$  and so on, in Fig. 5), each of which is capable of combining reversibly with a corresponding site ( $A_1, A_2$  and so on) on an actin molecule in the thin filament. A single  $M-A$  attachment allows variation of  $\theta$  (rotation in the plane of the diagram of Fig. 5) without hindrance, but no other degree of freedom of the myosin head relative to the actin molecule. (3) The affinity between these myosin and actin sites is smallest for  $M_1A_1$ , larger for  $M_2A_2$  and so on. (4) The sites are placed so that the myosin head has  $(s-1)$  stable positions, each of which allows two consecutive  $M$  and  $A$  sites to be attached simultaneously. (5) When the myosin head is in its  $(s-1)$ th stable position it can be detached from the thin filament by a process involving the hydrolysis of ATP.

On this basis the quick tension recovery is due to the tendency for the myosin head to rotate to positions of lower potential energy, while the fact that the recovery occurs at a finite speed is a manifestation of the rate constant for movement of the system from one of the stable positions to the next.

## Potential Energy Diagram of a Cross-bridge

Curves i-iv in Fig. 6 show the potential energy diagrams for individual attachment sites ( $M_1A_1, M_2A_2$  and so on) on a single cross-bridge. Each contains a flat-bottomed well extending over the range of myosin head positions where that particular attachment can exist. Curve v is the sum of curves i-iv, and therefore gives the total potential energy of the cross-bridge (in the absence of force in the link  $AB$ ): it consists of a series of steps, separated by narrow troughs at the positions where two of the links are attached simultaneously. The depth of each trough will depend on the shapes, and on the exact positions, of the sides of the potential wells that contribute to it; it is assumed in Fig. 6 that these are such that the quantities  $E_1$  and  $E_2$  (v, Fig. 6) are the same for each of the troughs.

The total potential energy of an attached cross-bridge contains also the potential energy of stretching the elastic link  $AB$ . The latter term is shown in curve vi, and the total in curve vii.

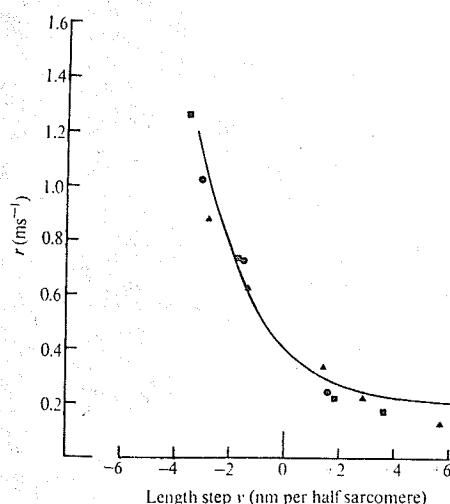


Fig. 4 Rate constant  $r$  of quick recovery phase following a length step of magnitude  $y$  (positive for stretch). Estimated as  $(\ln 3)/t_{1/3}$  where  $t_{1/3}$  is the time for recovery from  $T_1$  to  $(2T_2 + T_1)/3$  (see Fig. 3). From three experiments using the "spot-follower" device; temperature  $4^\circ\text{C}$ . The curve is  $r = 0.2(1 + \exp -0.5y)$ .

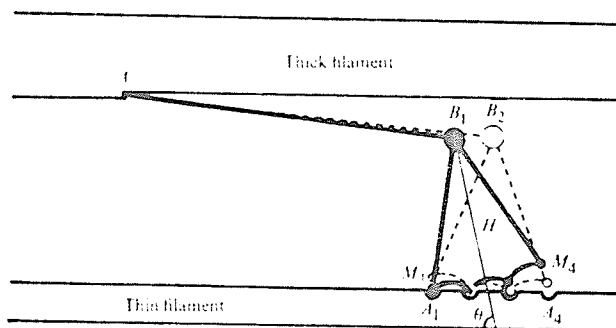


Fig. 5 Diagram showing assumed cross-bridge properties. The myosin head  $H$  is connected to the thick filament by a link  $AB$  containing the undamped elasticity which shows up as  $T_1$  (Fig. 3) in the whole fibre. Full line shows head in position where  $M_1A_1$  and  $M_2A_2$  attachments are made; broken lines show position where  $M_2A_2$  and  $M_3A_3$  attachments are made.

## Responses Expected Theoretically

In the mathematical section at the end of this article, we derive equations describing the response of a system of this kind to a step change of length. The system treated there is simplified by assuming that only two stable positions are available to each attached cross-bridge. The corresponding potential energy diagram is sketched in Fig. 7. This shows that  $B_2$ , the activation energy for transfer of a bridge from position 1 to position 2, contains a term  $H$  which depends on the force in the link  $AB$ , being increased by a stretch and reduced by a release.  $B_1$ , however, the activation energy for the reverse transfer, contains no such term and is independent of the force. It is this asymmetry which enables the theory to account for the way in which the rate constant of the quick tension recovery varies with the direction and magnitude of the length step: the theoretical result is expressed in equation (12) which is identical in form with equation (1), already shown (Fig. 4) to represent adequately the experimental data. The theory also leads to equation (16) for the tension level approached at the end of the quick recovery phase; this is plotted in Fig. 8 which is seen to reproduce the main features of the experimental  $T_2$  curve in Fig. 3.

The two striking features of the quick tension recovery are thus accounted for by this theory. The numerical values used in obtaining this degree of agreement are:  $E_1 - E_2$ , the potential energy difference between the stable positions of attachment of a cross-bridge, is equal to  $4 kT$ ;  $h$ , the travel of point  $B$  between its two stable positions, is 8 nm;  $K$ , the stiffness of the link  $AB$ , is  $2.5 \times 10^{-4} \text{ N m}^{-1}$ .

The following considerations show, however, that the assumption that the cross-bridge movement takes place in a single step is probably not correct.

**Isometric force and number of bridges.** Equations (4) and (7) show that the isometric force per attached cross-bridge is  $(E_1 - E_2)/h$ ; with the values mentioned in the last section this amounts to  $2.0 \times 10^{-12} \text{ N}$ . To reach a total force of  $3 \times 10^5 \text{ N m}^{-2}$ , such as real fibres produce, would therefore need  $1.5 \times 10^{17}$  attached bridges  $\text{m}^{-2}$  in each half-sarcomere. This is about 1.5 times greater than the number of myosin molecules present. The discrepancy would be greater if the number of cross-bridges were equal to the number of projections on the thick filaments detected by low-angle X-ray diffraction since this appears to be about half the number of myosin molecules<sup>15</sup>, and greater still if a substantial proportion of the cross-bridges were unattached during isometric contraction. (It is conceivable that each of the two heads on a myosin molecule should be counted separately; this would be appropriate only if the instantaneous elasticity existed within each of the heads, allowing them to shift independently.)

**Work per attached cross-bridge.** An upper limit to the external work done by the fibre per cross-bridge attachment will be given by the integral in equation (17), between the

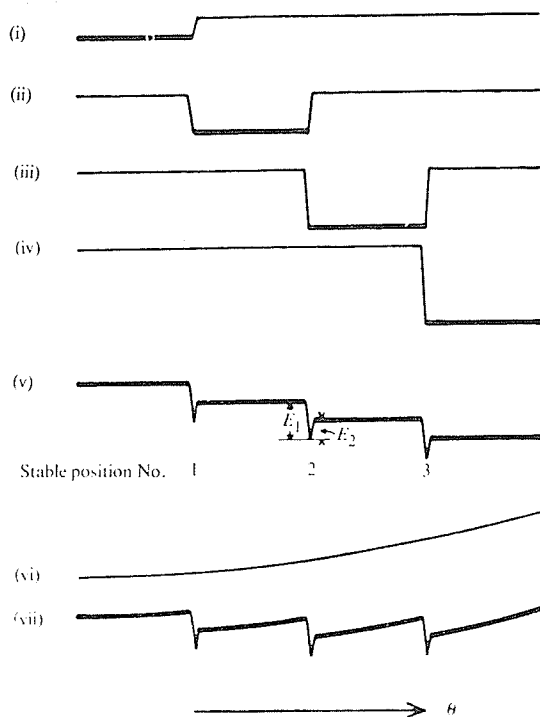


Fig. 6 Potential diagrams relating to the system illustrated in Fig. 5. i-iv, Diagrams for individual attachments  $M_1A_1$ ,  $M_2A_2$ ,  $M_3A_3$ ,  $M_4A_4$  respectively; in each the thick line corresponds to the range of  $h$  within which the corresponding  $M$  and  $A$  sites are attached; v, sum of i-iv, giving potential energy of a system composed only of a myosin head and a thin filament; vi, potential energy due to stretching the elastic link  $AB$ ; vii, total potential energy.

isometric point  $y=0$  and the point ( $y=-12.0$  nm) where  $\phi_2=0$ . With the adopted values of  $a$  and  $h$ , this is  $3.8$   $kT$ . This result is only about half the value which can be calculated as follows from the actual performance of frog muscle. Work can be as much as 40% of (work + initial heat)<sup>16</sup>, and the latter quantity is about 11 kcalories/mol<sup>1</sup> of phosphorylcreatine split<sup>17</sup>, giving the work term as 4.4 kcalories/mol<sup>1</sup>. This is equal to 7.3  $kT$  per molecule, which will represent the work per cycle of attachment and detachment of a cross-bridge if it is assumed that the cycle is coupled (presumably through ATP) to the hydrolysis of one molecule of phosphorylcreatine.

**Probable number of stable positions.** The quantitative treatment just presented has thus led to low values for the force and work per cross-bridge. It is just possible that revised values for  $a$  and for the number of cross-bridges will resolve these discrepancies, but it seems to us more likely that it will be necessary to assume that the cross-bridge movement takes place not in a single step but in two or perhaps more. This would lead to proportional increases in the calculated force and work, but the expected time course and extent of the quick tension recovery, which are already in good agreement with the experimental results, would not be much altered if each step has the same height  $E_1 = E_2$  as has already been assumed and the value of  $h$  is reduced so as to keep the same total range of travel. Fig. 5 is drawn for the case where the number of steps is 2 (3 stable positions and 4 points of attachment), which at present seems the most probable number.

## Relation to Earlier Theories

The idea of applying Fyring's theory of polymers to muscle is not new. A comprehensive theory of muscle was developed by Polissar<sup>18</sup>, in which the shortening of links in actomyosin chains was influenced in this way by the load, but this theory lost its relevance when it became clear that major changes of length take place by sliding, not folding, of the filaments.

The proposal that the sliding movement is generated by the tendency of attachments between the filaments to move through a series of a few positions of progressively lower potential energy was made many years ago by H. H. Weber<sup>19</sup>, who also pointed out that in this case the rate constants for shifting from one position to another would be affected by the force on the attachment. He discussed this idea purely on the basis of a translational movement of the thick relative to the thin filament, with a site rigidly fixed to one of the filaments transferring itself from one to the next of the sites on the other filament to which it could be attached. It is difficult to visualize a mechanism of this kind operating over the rather large distances—several nanometres—that the transient responses show to be involved, but the difficulty disappears if there is an elastic structure allowing one of the attachment sites to undergo substantial displacements relative to the filament to which it belongs.

On the kinetic side, the scheme discussed here combines the advantages of the proposals made by A. F. Huxley<sup>20</sup> in 1957 and by Podolsky *et al.*<sup>3</sup>. In each of these schemes the production of force was assumed to occur as an immediate consequence of the formation of a myosin-actin link. In A. F. Huxley's scheme, attachment was assumed to be the main rate-limiting factor in steady shortening, while detachment after the performance of work by a cross-bridge was relatively rapid; with these assumptions it is possible to fit A. V. Hill's relations between load, speed and heat production but not the transient responses discussed here. Podolsky *et al.* reversed the assumptions about the rate constants, making attachment rapid and breakage rate-limiting; in this way they were able to fit many aspects of transient responses but, as they recognized, not the thermal data. With appropriate rate constants for the initial attachment and final detachment of each cross-bridge, the present scheme can probably account for the force-velocity and thermal relationships in the same way as A. F. Huxley's 1957 scheme, while the rapid transfer between stable positions of the myosin head produces transient responses not unlike those which, on the theory of Podolsky *et al.*, result from the rapid formation of new attachments. The present proposal is able to combine the successful aspects of both of these theories because it subdivides the force-generating event into distinct stages, one for attachment and others for stretching the cross-bridge, the latter being much more rapid than the former. This separation also removes another difficulty that both of the earlier theories would very likely have met in a fully quantitative treatment. They assumed that tension is already present in the cross-bridge when it attaches to the thin filament; thermal motion would so seldom bring the cross-bridge to such a large deflexion that it might be impossible to account in that way for the rapidity of contraction that some real muscles achieve.

## Mathematical Section

Equations will be derived for the extent and time-course of the quick tension recovery to be expected from a system

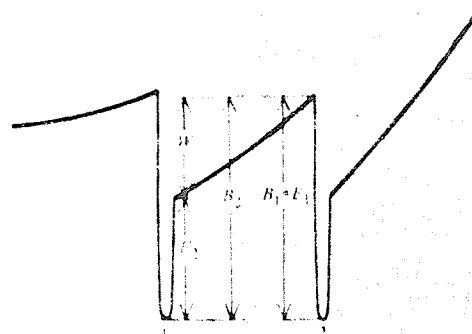


Fig. 7 Potential energy diagram equivalent to Fig. 6 (vii) but referring to the simplified system with only two stable positions.

similar to that shown in Fig. 5 but with only two instead of three stable positions of the myosin head relative to the thin filament. The following additional simplifying assumptions are also made. (1) Actual detachment and re-attachment of cross-bridges are slow enough to be disregarded. (2) Filaments themselves are completely rigid. (3) Filaments undergo no sliding movements except when the total length of the fibre is being altered. (4) The elasticity of the link  $AB$  obeys Hooke's law. (5) The link  $AB$  is capable of exerting negative as well as positive tensions. (6) In the isometric steady state, every attached cross-bridge spends equal amounts of time in each of the two available positions (this cannot be strictly true in real muscle because the spacings along the thick and thin filaments are not in any simple ratio, so the relative positions of the myosin and actin molecules must vary from one cross-bridge to another). (7) The time taken in transferring from one to the other of the two positions is negligible.

The following notation will be used;  $n_1$ : fraction of attached bridges in position 1;  $n_2$  ( $=1-n_1$ ): fraction of attached bridges in position 2;  $y$ : displacement of thick relative to thin filament when fibre is stretched or shortened (zero in isometric state before the applied length change; positive for stretch);  $y_0$ : extension of elastic link  $AB$  when bridge is midway between positions 1 and 2 (equal to amount of sudden sliding movement needed to bring tension to zero from the isometric state);  $h$ : increase in length of  $AB$  when bridge shifts from position 1 to position 2;  $K$ : stiffness of link  $AB$  (assumed to obey Hooke's law);  $F_1$ : tension in  $AB$  when bridge is in position 1;  $F_2$ : tension in  $AB$  when bridge is in position 2;  $\phi$ : time average of  $F_1$  and  $F_2$ .

From these definitions,

$$F_1 = K(y + y_0 - h/2) \text{ and } F_2 = K(y + y_0 + h/2) \quad (2)$$

and the time average of tension is

$$\phi = n_1 F_1 + n_2 F_2 = K(y + y_0 - h/2 + hn_2) \quad (3)$$

In the isometric state,  $y=0$  and  $n_2=1/2$ , and this equation reduces to the expression for the isometric force per attached cross-bridge

$$\phi_0 = Ky_0 \quad (4)$$

The rate constants  $k_+$  for transfer from position 1 to position 2, and  $k_-$  for transfer from 2 to 1, are governed by the energy barriers  $B_2$  ( $=E_2+W$ ) and  $B_1$  ( $=E_1$ ) respectively (Fig. 7).  $W$  is the work done in stretching  $AB$  when the bridge transfers from position 1 to position 2, and is given by

$$W = h \frac{F_1 + F_2}{2} = Kh(y + y_0) \quad (5)$$

from equations (2).

Assuming the  $k$ s proportional to  $\exp -B/kT$ , we have

$$\begin{aligned} k_+ &= k_- \exp (B_1 - B_2)/kT \\ &= k_- \exp (E_1 - E_2 - W)/kT \\ &= k_- \exp (E_1 - E_2 - Kh(y + y_0))/kT \end{aligned} \quad (6)$$

where  $k_-$  is constant since  $B_1$  is a fixed quantity independent of the tension in  $AB$ .

In the isometric state we have assumed  $n_1=n_2$ , so  $k_+=k_-$ ; also  $y=0$  since  $y$  is defined as a length change from the isometric state. It then follows from (6) that

$$E_1 - E_2 = Khy_0 \quad (7)$$

and (6) becomes

$$k_+ = k_- \exp -y.Kh/kT \quad (8)$$

In the experiments we are considering,  $y$  is suddenly altered by imposing a length change on the muscle fibre, and is sub-

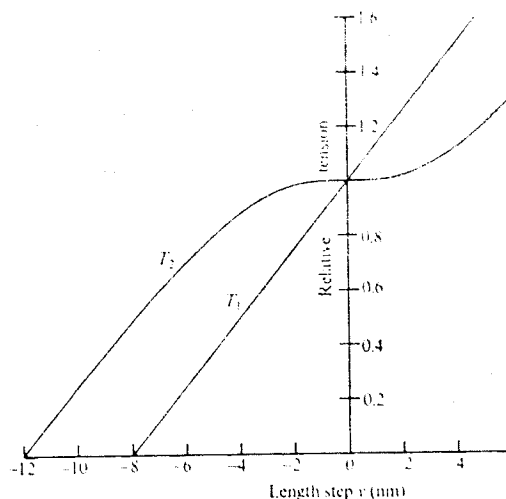


Fig. 8 Curves of  $T_1$  and  $T_2$  calculated from the simplified system, plotted on same scales as the experimental values in Fig. 3.  $T_2$  curve: Equation (15) with  $E_1 - E_2 = 4kT$ ,  $1/a = 2$  nm,  $h = 8$  nm.

sequently held constant. The transfer of myosin heads from one position to the other is then governed by the equation

$$\begin{aligned} dn_2/dt &= k_+ n_1 - k_- n_2 \\ &= k_+ - (k_+ + k_-) n_2 \end{aligned} \quad (9)$$

This equation represents an exponential approach, with rate constant  $r$  given by

$$r = k_+ + k_- \quad (10)$$

towards an equilibrium where

$$n_2 = k_+ / (k_+ + k_-) \quad (11)$$

Substituting from (8) into (10) we have

$$r = k_- (1 + \exp -y.Kh/kT) \quad (12)$$

This has the same form as equation (1), and the equations become identical, giving approximate agreement with the experimental results in Fig. 4, if we take

$$Kh = \alpha kT \quad (13)$$

Equation (8) can therefore be written

$$k_+ = k_- \exp -\alpha y \quad (14)$$

and (11) becomes

$$n_2 = \frac{1}{2} \left( 1 + \tanh \frac{\alpha y}{2} \right) \quad (15)$$

The tension  $\phi_2$  at the end of the quick recovery (corresponding to  $T_2$  in the whole fibre) is obtained by combining (3), (13) and (15) to give

$$\phi_2 = \frac{\alpha kT}{h} \left( y_0 + y - \frac{h}{2} \tanh \frac{\alpha y}{2} \right) \quad (16)$$

The work done during shortening at a low enough speed so that  $n_2$  always has its equilibrium value would be obtained by integrating (16):

$$\int \phi_2 dy = kT \left( \frac{\alpha y}{h} \left( y_0 + \frac{y}{2} \right) - \ln \cosh \frac{\alpha y}{2} \right) \quad (17)$$

To match the points in Fig. 4,  $\alpha$  is taken as  $5 \times 10^8 \text{ m}^{-1}$ , the value used for the curve in that figure. ( $E_1 - E_2$ ) is shown by equations (7) and (13) to be equal to  $\alpha y_0 kT$ . From Fig. 3 (broken line),  $y_0$  is about 8 nm, giving  $E_1 - E_2 = 4kT$ .  $h$  has to be chosen to give the right shape for the curve of  $T_2$  against  $y$  (equation 15). A value  $4/\alpha$ , or 8 nm, is used in Fig. 8; lower values give a less inflected curve and higher values give a curve with a region of negative slope.

## Generation of Tension

The tension changes observed in the first few milliseconds after suddenly changing the length of an active muscle fibre suggest the following mechanism for the generation of tension or shortening by the cross-bridges. Each cross-bridge has three stable positions with progressively lower potential energies, in steps of about 4 times  $kT$ , separated by about 4 nm of travel. Transfer from one of these positions to the next is made possible, without simultaneous displacement of the whole filaments through an equally large distance, by the presence of elasticity associated with each individual cross-bridge. The tension generated in this way in the elastic element will show up as such if the muscle length is held constant, or will help to make the filaments slide past each other if shortening is permitted.

A simplified theoretical treatment is given; a more complete treatment will be presented later.

Received August 25, 1971.

- <sup>1</sup> Podolsky, R. J., *Nature*, **188**, 666 (1960).
- <sup>2</sup> Civan, M. M., and Podolsky, R. J., *J. Physiol.*, **184**, 511 (1966).
- <sup>3</sup> Podolsky, R. J., Nolan, A. C., and Zaveler, S. A., *Proc. US Nat. Acad. Sci.*, **64**, 504 (1969).
- <sup>4</sup> Huxley, A. F., and Simmons, R. M., *J. Physiol.*, **208**, 52P (1970).
- <sup>5</sup> Gordon, A. M., Huxley, A. F., and Julian, F. J., *J. Physiol.*, **184**, 143 (1966).
- <sup>6</sup> Huxley, A. F., and Simmons, R. M., *J. Physiol.*, **197**, 12P (1968).
- <sup>7</sup> Gasser, H. S., and Hill, A. V., *Proc. Roy. Soc., B*, **96**, 398 (1924).
- <sup>8</sup> Hill, A. V., *Proc. Roy. Soc., B*, **141**, 104 (1953).
- <sup>9</sup> Jewell, B. R., and Wilkie, D. R., *J. Physiol.*, **143**, 515 (1958).
- <sup>10</sup> Huxley, A. F., and Simmons, R. M., *J. Physiol.*, **218**, 59P (1971).
- <sup>11</sup> Eyring, H., *J. Chem. Phys.*, **4**, 283 (1936).
- <sup>12</sup> Burte, H., and Halsey, G., *Tex. Res. J.*, **17**, 465 (1947).
- <sup>13</sup> Davies, R. E., *Nature*, **199**, 1068 (1963).
- <sup>14</sup> Huxley, H. E., *Science*, **164**, 1356 (1969).
- <sup>15</sup> Huxley, H. E., *J. Mol. Biol.*, **7**, 281 (1963).
- <sup>16</sup> Hill, A. V., *Proc. Roy. Soc., B*, **127**, 434 (1939).
- <sup>17</sup> Wilkie, D. R., *J. Physiol.*, **195**, 157 (1968).
- <sup>18</sup> Polissar, M. J., *Amer. J. Physiol.*, **168**, 766, 782, 793 and 800 (1952).
- <sup>19</sup> Weber, H. H., *The Motility of Muscle and Cells*, 32 (Harvard University Press, Cambridge, Massachusetts, 1958).
- <sup>20</sup> Huxley, A. F., *Prog. Biophys.*, **7**, 255 (1957).

# How Dextrous was Neanderthal Man?

JONATHAN H. MUSGRAVE

Department of Anatomy, The Medical School, University Walk, Bristol BS8 1TD

**Results of multivariate statistical analyses indicate that the bones of the hand of Neanderthal man were metrically and morphologically unique and that he may not have been as dextrous as living *Homo sapiens*.**

THE postcranial skeleton of Neanderthal man has been studied less intensively than his skull. This is to be regretted because any serious attempt to re-assess the phylogenetic status of the Neanderthals must be based on their total morphological pattern<sup>1</sup> and not solely on evidence of cranial variation. In an attempt to rectify this situation I have made a detailed study of as many as possible of the Neanderthal hand bones listed by Vallois and Movius<sup>2</sup>. Measurements were taken on these bones and on comparative samples of European Upper Palaeolithic, Mesolithic and modern hand bones. These measurements and indices calculated from them were then submitted to discriminant function (canonical variate) analyses and Mahalanobis's  $D^2$  tests<sup>3</sup>. This article presents some of the conclusions drawn from this investigation<sup>4</sup>.

## Thumb

(1) The metacarpal seems to have been neither relatively nor absolutely short, as earlier workers had suggested<sup>5,6</sup>, and it was instead the great transverse width of the head, a feature which had also aroused comment<sup>7,8</sup>, which proved to be the most important dimension. This observation may be correlated with a very noticeable anatomical feature, a flange which runs up the distal half of the radial side of the shaft (Fig. 1). Into this was inserted opponens pollicis muscle, clearly large and powerful in Neanderthal man<sup>9</sup>, a suggestion which is

in keeping with recent theories on the role of this muscle as an abductor of the thumb in a firm grip<sup>10</sup>. Associated with this flange is a marked depression<sup>8</sup> diagonally opposite, from which arose the first metacarpal head of the first dorsal interosseous, another "power" muscle.

Other unusual features of the Neanderthal thumb metacarpal include an asymmetry in the transverse curvature of the head and the presence in several specimens of a condyloid rather than a saddle-shaped proximal articular surface. This asymmetry has been noted in some non-human primate genera<sup>11,12</sup> and may reflect difficulties in opposing the thumb to the other digits. The condyloid articular surface, clearly visible in the specimen from La Chapelle-aux-Saints<sup>5</sup> but only partly developed in those from Kiik-Koba<sup>9</sup> and La Ferrass

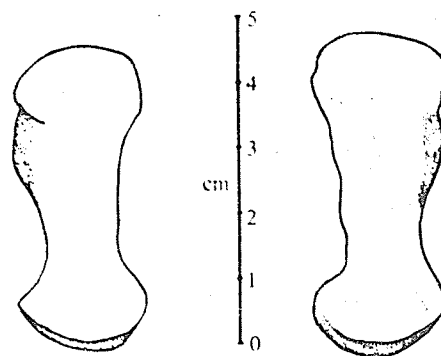


**Fig. 1** Palmar aspect of Neanderthal thumb metacarpals. The principal features are: (1) the radially projecting ridge (stippled) into which was inserted opponens pollicis muscle; (2) the asymmetry of the curve of the distal articular surface; and (3) the narrow waist at the proximal end of the shaft, formed on the ulnar side by the impression for the origin of the first metacarpal head of the first dorsal interosseous muscle. Both specimens belonged to male Neanderthals. Tracings were made from photographs of casts.